

**MODELING OF GRID CONNECTED PV ARRAY USING
SIMULINK/MATLAB**

Thesis submitted for partial fulfillment of requirements for the degree of

MASTER OF ELECTRICAL ENGINEERING

By

TANMOY DUTTA

(UNIVERSITY ROLL NO. 001410802008)

EXAM ROLL NO. M4ELE1607

Reg. No. 128895 of 2014-15

Under the Guidance and Supervision of

Asst. Prof. Ayan Kumar Tudu

Department of Electrical Engineering

Faculty of Engineering and Technology

JADAVPUR UNIVERSITY

Kolkata 700032, India

2014-2016

JADAVPUR UNIVERSITY
KOLKATA-700032

FACULTY OF ENGINEERING AND TECHNOLOGY

Department of Electrical Engineering

Certificate for Recommendation

This is to certify that Shri. Tanmoy Dutta has completed his project work entitled “**Modeling of Grid Connected PV array using SIMULINK/MATLAB**” under our direct supervision and guidance. This thesis is submitted in partial fulfilment of the requirements for the award of degree of Master of Electrical Engineering during the academic year 2014-2016.

Supervisor

Asst. Prof. Ayan Kumar Tudu

Department of Electrical Engineering
Jadavpur University, Kolkata- 700032

Countersigned by

Prof. (Dr.) Swapan Kumar Goswami
Head, Department of Electrical Engineering
Jadavpur University, Kolkata- 700032

Prof. Sivaji Bandyopadhyay
Dean, Faculty of Engineering and Technology
Jadavpur University, Kolkata- 700032

JADAVPUR UNIVERSITY

Kolkata-700032, India

FACULTY OF ENGINEERING AND TECHNOLOGY

*Certificate of Approval**

The foregoing THESIS is thereby approved as a creditable study of an Engineering Subject carried out and presented in a manner satisfactory to warrant its acceptance as a pre-requisite to the DEGREE for which it has been submitted. It is notified to be understood that by this approval, the undersigned do not necessarily endorse or approve any statement made, opinion expressed and conclusion drawn therein but approve the THESIS only for the purpose for which it has been submitted.

FINAL EXAMINATION FOR
EVALUATION OF THE THESIS

BOARD OF EXAMINERS

.....
.....
.....
.....

* Only in case the thesis is approved

(Signature of Examiners)

Declaration of Originality and Compliance of Academic Ethics

I hereby declare that this thesis contains literature survey and original research work by the undersigned candidate, as part of their “**Master of Engineering in Electrical Engineering**” studies.

All information in this document have been obtained and presented in accordance with academic rules and ethical conduct.

I also declare that, as required by these rules and conduct, I have fully cited and referenced all materials and results that are not original to this work.

Name : **TANMOY DUTTA**

Examination Roll Number : **M4ELE1607**

Thesis Title : **Modeling of Grid Connected PV array
using SIMULINK/MATLAB**

Signature with Date :

ACKNOWLEDGEMENT

It is a pleasant task to express my gratitude to all those who have assisted me in my project work.

First of all I take this opportunity to express my sincere thanks and deepest sense of gratitude to my guide Asst. Prof. Ayan Kumar Tudu of Electrical Engineering Department for offering his guidance to me in carrying out this project. I would like to thank him for providing me with his valuable time and helpful suggestions. He also helped me by providing constructive ideas throughout the tenure of this work.

I am indebted to Prof. Dr. Swapan Kumar Goswami, Head, Department of Electrical Engineering, Jadavpur University, for providing me with all the necessary facilities for carrying out this work.

I would also like to convey my gratitude to Prof. Dr. Subrata Paul, Dr. Sunita Halder nee Dey, Dr. Sudipta Debnath and Asst. Prof. Madhumita Mandal of Department of Electrical Engineering, Jadavpur University for their guidance, encouragement and valuable suggestions in the course of this work.

I would like to express my heart-felt gratitude to my parents and my family members for their love and active support throughout the endeavor.

Last, but not the least, I would like to thank my batch-mates and PhD researchers, who have directly or indirectly helped me in this work.

Tanmoy Dutta
Electrical Engineering Department
Jadavpur University
Kolkata- 700032
May 30, 2016.

CONTENTS

CHAPTERS	PAGE NO.
CHAPTER 1	
INTRODUCTION	1-5
1.1 Motivation of the Thesis	1-2
1.2 Literature Review	2-4
1.3 Problem Statement	4
1.4 Thesis Organization	5
CHAPTER 2	
MODELING OF PHOTOVOLTAIC DEVICES	6-17
2.1 The Photovoltaic Cell	6-7
2.2 The Photovoltaic Module	8-9
2.3 Modeling of Photovoltaic Array	10
2.4 Simulink Model	11-13
2.5 Validation of the Model	13-17
CHAPTER 3	
MAXIMUM POWER POINT TRACKING	18-24
3.1 MPPT Algorithm	18-19
3.2 Perturb & Observe (P&O) Method	19-21
3.3 Incremental Conductance (INC) Method	21-24

CHAPTER 4	
DC-DC BOOST CONVERTER	25-29
4.1 Continuous Conduction Mode (CCM)	27
4.2 Discontinuous Conduction Mode (DCM)	28-29
CHAPTER 5	
INVERTER TOPOLOGY	30-38
5.1 Comparison between CSI & VSI	32-33
5.2 Voltage Sourced Converter (VSC)	33-34
5.3 Control of VSC	34-38
CHAPTER 6	
SIMULATION AND RESULTS	39-55
6.1 Simulation of MPPT Algorithms	39-40
6.2 Simulation of Boost Converter	40-41
6.3 Voltage Source Converter	41-42
6.4 Interfacing with AC Power Supply	42-44
6.5 Result & Discussion	48-50
CHAPTER 7	
CONCLUSION AND SCOPE OF FUTURE WORK	51-52
7.1 Conclusion	51
7.2 Future Scope of Work	51-52
BIBLIOGRAPHY	53-56
APPENDIX A	
MANUFACTURER'S DATASHEET	57-59

CHAPTER 1

Introduction

1.1 Motivation of the Thesis

In recent years energy demand is increasing across the world. More number of generating stations are to be constructed to meet this demand. The use of fossil fuels deteriorate ecological environment and causes global warming. Now it is become a big challenge to societies around the world to fulfill the energy demand keeping minimum damage to environment. In this circumstances use of non-conventional energy has emerged as a solution to this problem. It is clean as the CO₂ emission is very low and also 'renewable'.

Recent years have seen remarkable technological development in the field of renewable energy. Energy sources like solar, wind, tidal, geothermal are the main sources which are used as a renewable energy sources. Countries like China and USA are heavily investing in solar, wind and biofuels. At present around 30 nations in the world are using renewable energy to meet about 20 percent of their total energy demand. Norway and Iceland, the two countries who have generated all their electricity using renewable energy sources.

1.1.1 SOLAR ENERGY

Among the various sources of renewable energy, the electrical energy obtained from solar energy is currently regarded as a natural energy source which is most useful since it is free, abundant, clean, and distributed over the Earth and participates as a primary factor of all other processes of energy production on Earth. PV systems have been started to be used widely in domestic electricity supply. In fact growth of PV panels for electricity generation is one of the highest in the field and this tendency is expected to continue in the coming few years. Under solar irradiation solar panel converts sunlight into electrical energy by photovoltaic effect. It was first observed by A. E Becquerel in 1839 [15].

1.1.2 SOLAR ENERGY IN INDIA

Geographically India being a tropical country receives adequate solar radiation for 300 days, which amounts to 3000 hours of sunlight equivalent to over 5000 trillion kWh. Due to lack of

electricity infrastructure a major section of its populace is still off grid. Especially in rural area 18000 villages could not be electrified through conventional grid system. Development in solar energy could be the best alternatives to electrify the rural and urban area. Currently India has around 1.2 million solar home lighting systems and is also India ranked the number one in Asia for solar off-grid products. As of 31 December 2015 the installed grid connected solar power capacity is 4,879.00 MW, and India expects to install an additional 10,000 MW by 2017 [2].

The work presented in this thesis is to represent a model of PV power generating system connected to utility grid using Matlab/Simulink. In the proposed model a DC-DC boost converter is used with the necessity MPPT control method and is interfaced with the grid through a voltage sourced inverter. Each chapter in this thesis will explain the specific area of research.

1.2 Literature Review

For the successful execution of the thesis work it is very important to discuss about the various types of existing work that has been done in this domain and ponder upon the proposed improvement possible. In the literature review some important parts related to this are discussed.

Modeling of Photovoltaic Devices

As the name implies photovoltaic device is the key part of any Photovoltaic System. Due to the low voltage generated in a PV cell, a number of PV cells are connected in series and parallel to form a PV module for desired output. Lots of work has already been done in this topic, some of which are briefly presented here.

Michael E. Ropp [13] presented a MATLAB/SIMULINK model of a single-phase grid connected PV system suitable for system-level investigations. Simplified means for modeling the PV array and integrating a gradient based MPPT into a very simple average model of the power converter are developed, and the model has been experimentally tested.

Habbati Bellia et al [11] presented a detailed modeling and simulation of the PV cell and module. It is implemented under MATLAB/SIMULINK environment. The chosen model is the single diode model with both series and parallel resistors for greater accuracy.

I. H. Atlas et al [10] developed a photovoltaic array simulation model to be used in MATLAB/SIMULINK software. The model is developed using the basic circuit equations of the photovoltaic solar cell including the effects of solar irradiance and temperature changes. The PV cell output voltage is a function of the photocurrent that is mainly determined by load current depending on the solar irradiance level during the operation.

Shivananda Pukhrem in [15] proposed a circuit based simulation model for a PV cell for estimating the IV characteristic curves of photovoltaic panel with respect to changes in environmental parameters and cell parameters. Considering these two the author developed a model in MATLAB/SIMULINK with a variable load resistance at the output.

Tarak Salmi et al [29] focused on a Matlab/Simulink model of a photovoltaic cell. The model is based on mathematical equations and is described through an equivalent circuit including a photocurrent source, a diode, a series resistor and a parallel resistor. The developed model allows the prediction of PV cell behavior under different physical and environmental temperature and solar radiation.

1.2.1 DC-DC Boost Converter

It is also known as a step up converter. The typical application is necessary to increase the output voltage of the PV array as the output of the PV array is less than what has to be supplied to the consumers. In this regard some research has been done and can be found in the following papers.

Hassan Fathabadi [23] proposed a novel high efficiency DC/DC boost converter to be used in PV systems. The converter includes only one metal oxide semiconductor field effect transistor (MOSFET) switch, and two diodes. It is shown theoretically and experimentally that the only switch of the converter is turned on and turned off respectively under zero current switching (ZCS) and zero voltage switching (ZVS) conditions, and the two diodes are turned on/off under ZCS condition, so there are no switching losses.

B. M Hasaneen et al [24] proposed a design and simulation of DC/DC boost converter. The input is usually from a PV array and therefore the design and simulation in this paper covers the whole range of radiations and temperature. In this paper they analyze the equations of a boost converter and propose the design components of DC/DC boost converter. This work is applied to photovoltaic system for tracking the point of maximum power.

P. Sathya et al [25] presented the design and implementation of high performance closed loop Boost converter for solar powered LED lighting system. The proposed system consists

of solar photovoltaic module, a closed loop boost converter and LED system. The closed loop boost converter is used to convert a low level dc input voltage from solar PV module to a high level dc voltage required for the load.

1.2.2 Maximum Power Point Tracking (MPPT)

It is very important to track the maximum power point accurately under all operating conditions so that maximum available power is always obtained. Several distinct methods of MPPT are available in literature. A few of them are presented here.

Moacyr Aurliano Gomes de Brito et al [8] presented evaluations among the most usual maximum power point tracking (MPPT) techniques, doing meaningful comparisons with respect to the amount of energy extracted from the photovoltaic (PV) panel in relations to the available power, PV voltage ripple, dynamic response and use of sensors. Total work has been performed in Matlab/Simulink.

A.Safari et al [20] has presented incremental conductance method (INC) for maximum power point tracking (MPPT) using DC-DC cuk converter. Comprehensive analysis and simulation of KC85T solar module and equivalent electric circuit are provided while effects of various environmental conditions on the PV module behavior is investigated. In order to fully understand the PV module working specifications fundamental characteristics of PV cells are discussed.

Saravana Selvan. D [21] has proposed the study of incremental conductance MPPT algorithm. This can be experimentally verified by modeling the PV system with MPPT algorithm in Matlab/Simulink software. This paper reviews the basic characteristics of the PV cell and the simulation model of the circuit.

1.2.3 Power Electronic Interfacing with Utility Grid

Neng Cao, Yajun Cao and Jiaoyu Liu [26] have proposed an inverter control system whose advantage is its high speed and flexibility due to the application of advanced control algorithm. The source harmonic current is remarkably reduced for this design.

Yao-Nan Tong et al [27] presented a single-phase full bridge photovoltaic grid-connected inverter.

Amirnaser Yazdani et al [28] described a voltage sourced converter (VSC) in solar power system. This paper also deals with phase transformation and control of VSC.

1.3 Problem Statement

The above literature review shows the existing research for photovoltaic system. But still further investigations are needed on the design aspects of photovoltaic arrays, the maximum power point tracker and the power electronics interface between the PV system and grid. In this regard an attempt has been made in this work to address the above mentioned issues.

This thesis carried out a detailed study of photovoltaic systems. It incorporates analysis and developments work on modeling and simulation of the grid connected photovoltaic systems.

The well accepted software package MATLAB/SIMULINK for simulating power system components has been used. The thesis attempts

- To develop an accurate model of PV module and validate the same with a commercially available model of PV.
- To interface with a utility grid system using proper converter controls.
- Finally to confirm the effectiveness of the developed design with the help of simulation results.

1.4 Thesis Organization

- *Chapter 2* explains about the brief theory, required to understand the modeling of the solar PV module. The model, definition and array of solar cell is given. It also explains the development of the mathematical expressions that represent the electrical behavior of the solar cell. With the help of MATLAB/SIMULINK the model of solar cell has been developed and is validated with a commercially available PV module Sun power SPR-305 WHT.
- *Chapter 3* gives a brief discussion about the maximum power point tracking method.
- *Chapter 4* discuss the theory of DC-DC boost converter and its control.
- *Chapter 5* discuss the theory of voltage sourced converter and its control for three phase grid integrated PV system
- *Chapter 6* shows the simulation and results of the designed model.

And finally *Chapter 7* concludes the thesis and discuss about the future work in connection with a PV array connected to a grid.

CHAPTER 2

MODELING OF PHOTOVOLTAIC DEVICES

The Photovoltaic device is the heart of the PV system i.e. the main source of energy in the system. So it is very important to understand the working principle of a PV array. The ability to produce electrical energy by means of converting solar energy is called Photovoltaic property. A simple solar cell consists of solid state p-n junction fabricated from a semiconductor material. When sunlight hits the solar cell the energy from the photons creates free charges that are separated by the electrical field, creating a potential so that when a load is placed between the terminals of the PV module a photo current (IPV) is created. The most common material used in photocells today is silicon (Si) divided in mono-crystalline, polycrystalline, and amorphous forms. The amount of energy they can deliver changes depending on the material of the cell and the incidence of sunlight. To develop a model of solar cell it is important to evaluate the effect of different factors on the solar panels and to consider the characteristics given by the manufacturers in the datasheet. It is to be noted that to form a PV module, a set of cells are connected in series or in parallel. PV arrays are built up with combined series parallel combinations of several PV modules. Thus, the mathematical models for PV array can be attained from the equivalent circuit of the PV cells.

2.1 The Photovoltaic Cell

A simple equivalent circuit of a solar cell is a current source in parallel with a diode as seen in Fig. 2.1. The two parameters used to model and characterize a PV cell are: the open circuit voltage (V_{OC}) and the short circuit current (I_{SC}). The V_{OC} is the maximum voltage which a solar cell can provide at zero current. The I_{SC} is the maximum current which a solar cell can provide at zero voltage.

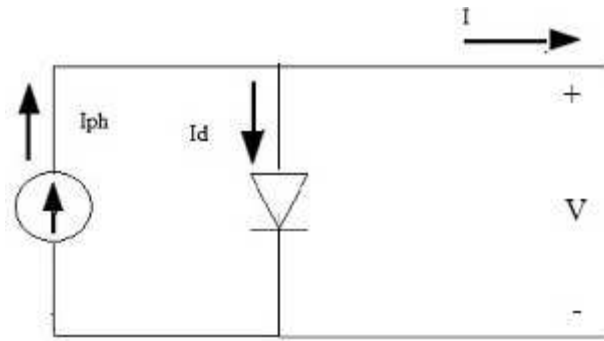


Fig. 2.1 Ideal single diode model

A diode is connected in anti-parallel with the light generated current source. The output current I is obtained by Kirchoff law:

$$I = I_{ph} - I_d \quad 2.1.1$$

Here I_{ph} is the photocurrent, I_d is the diode current. I_d is given by the following equation:

$$I_d = I_0 \left[\exp\left(\frac{V}{V_T}\right) - 1 \right] \quad 2.1.2$$

$$V_T = k \cdot T / q \quad 2.1.3$$

Where

- I_0 = reverse saturation current or leakage current
- V = diode voltage
- q = electron charge ($1.602 \times 10^{-19} \text{C}$)
- k = Boltzmann constant $1.381 \times 10^{-23} \text{J/K}$
- T = temperature (Kelvin)
- I = output current

Therefore combining the equations (2.1.1) & (2.1.2) yields

$$I = I_{ph} - I_0 \left[e^{\frac{qV}{kT_c}} - 1 \right] \quad 2.1.4$$

2.2 The Photovoltaic Module

A typical solar cell produces less than 0.5 V. Therefore to have adequate power output at suitable voltage level, cells are connected in series-parallel combination to form a PV module. The same basic modeling equations as in a PV cell are also followed by the module. The simple PV cell model neglects to take into consideration a series of parameters that create an accurate model. They are:

1. R_p : Parallel resistance that accounts for the loss associated with a slight leakage current through a parallel resistive path to the device. R_p is neglected in most of the models because its effect isn't noticeable unless a large amount of cells are connected in parallel.
2. R_s : Series resistance that accounts for any resistance in the current paths through the semiconductor material, the metal grid, contacts and currents controlling the system. This value also accounts for the loss associated with connecting a number of cells in series.
3. N_s : Number of PV cells connected in series
4. a : Diode ideality factor, is considered constant

Taking into all these additional elements mentioned above the equation 2.1.4 changes to

$$I = I_{PH} - I_0 \left[\exp\left(\frac{qV}{aN_s kT}\right) - 1 \right] - \frac{V + IR_s}{R_p} \quad 2.2.1$$

The equivalent circuit of a solar cell is depicted below.

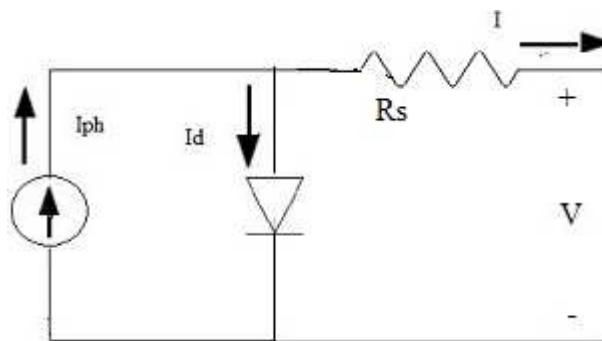


Fig. 2.2.1 Practical model with R_s

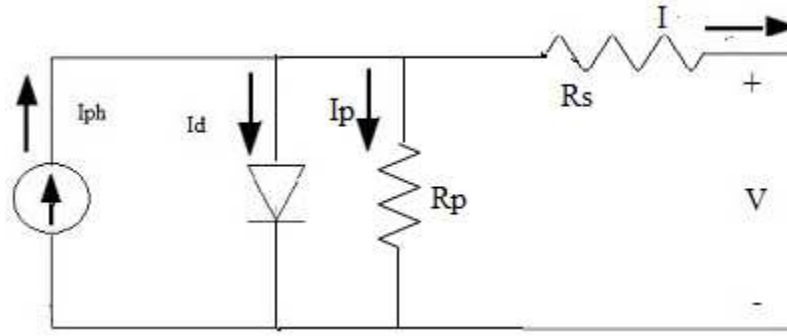


Fig. 2.2.2 Practical model with R_s and R_p

It is considered that parameters I_{ph} , I_0 , R_s , R_p are dependent on the incident solar irradiation and cell temperature [11]. The current generated by the solar cells IPV can be approximated with the short circuit current (I_{SC}).

The equation of the photocurrent can be written as:

$$I_{ph} = \left[I_{SC} + K_i (T - T_{ref}) \right] \frac{G}{G_{ref}} \quad 2.2.2$$

Where

- I_{SC} = is the light generated current
- K_i = co-efficient temperature of short circuit current per degree.
- T = Temperature in Kelvin
- T_{ref} = reference temperature in Kelvin
- G = irradiance (W/m^2)
- G_{ref} = nominal irradiance (usually $1000 W/m^2$)

The reverse saturation current I_0 of PV module is:

$$I_0 = I_{on} \left[\frac{T}{T_r} \right]^3 \exp \left[\left(\frac{qE_g}{ak} \right) \left(\frac{1}{T_r} - \frac{1}{T} \right) \right] \quad 2.2.3$$

In the above equation E_g is band gap energy of the semiconductor device and I_{on} is the saturation current.

$$I_{on} = \frac{I_{SC}}{\left[\exp \left(\frac{qV_{oc}}{N_s kaT} \right) - 1 \right]} \quad 2.2.4$$

2.3 Modeling of Photovoltaic Array

A PV Array is a collection of PV modules. It follows the same basic modeling equations. In literature [10, 11, 13, 16, 26 and 29] different types of PV models are developed. For the purpose of this research we will be using the method described in [11]. The model consists of finding the characteristic curve of the PV module from the datasheet. The manufacture's data sheet on PV modules usually provides the following parameters:

1. $V_{OC}(V)$: Open Circuit Voltage
2. $I_{SC}(A)$: Short Circuit Current
3. $V_{mp}(V)$: Voltage at maximum power point
4. $I_{mp}(A)$: Current at maximum power point
5. K_V : Temperature co-efficient of V_{OC}
6. K_i : Temperature co-efficient of I_{SC}
7. P_{mp} : Power at maximum point

In order to make the proposed model more credible, R_P and R_S are chosen so that the computed max power P_{mp} is equal to the experimental value $P_{mp,ex}$ at standard test condition (STC). So it is possible to write the next equation:

$$I_{mp,ref} = P_{mp,ref} / V_{mp,ref} = P_{mp,ex} / V_{mp,ref}$$

$$P_{mp,ex} = V_{mp} \left[I_{ph} - I_0 \left\{ \exp \left(\frac{V_{mp} + I_{mp} \cdot R_S}{a} \right) - 1 \right\} - \frac{V_{mp} + R_S \cdot I_{mp}}{R_P} \right] \quad 2.3.1$$

$$R_P = \frac{V_{mp} + I_{mp} \cdot R_S}{I_{sc} - I_0 \left\{ \exp \left[\frac{V_{mp} + R_S \cdot I_{mp} - V_{OC}}{a} \right] \right\} + I_{sc} \left\{ \exp \left(\frac{-V_{OC}}{a} \right) \right\} - \left(\frac{P_{mp}}{V_{mp}} \right)} \quad 2.3.2$$

The iteration starts at $R_S=0$ which must increase in order to move the modeled Maximum Power Point until it matches with the experimental MPP. The corresponding R_P is then computed.

2.4 Simulink Model

The simulation is performed using the Matlab/Simulink software. The matlab model of photovoltaic array is based on [11]. First modeling of equation 2.2.2 as seen in Fig 2.4(a) followed by modeling of equation 2.2.3 in fig 2.4 (b). The values of R_S and R_P were calculated from equation 2.2.1.

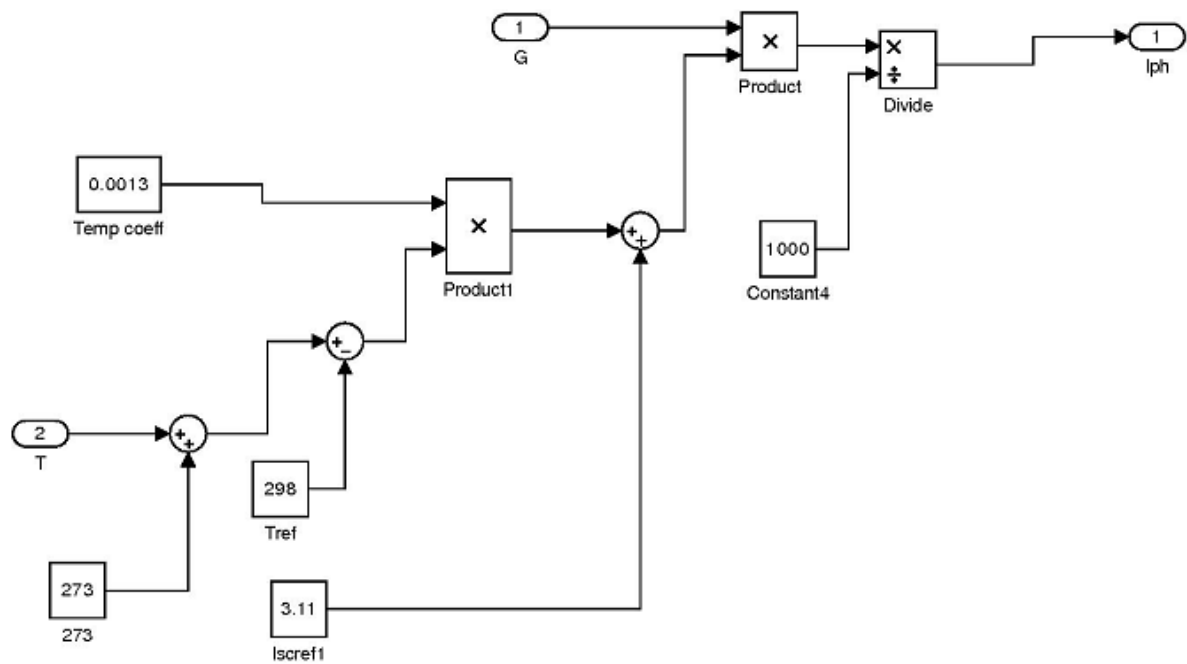


Fig. 2.4 (a) Detailed I_{ph} Implementation

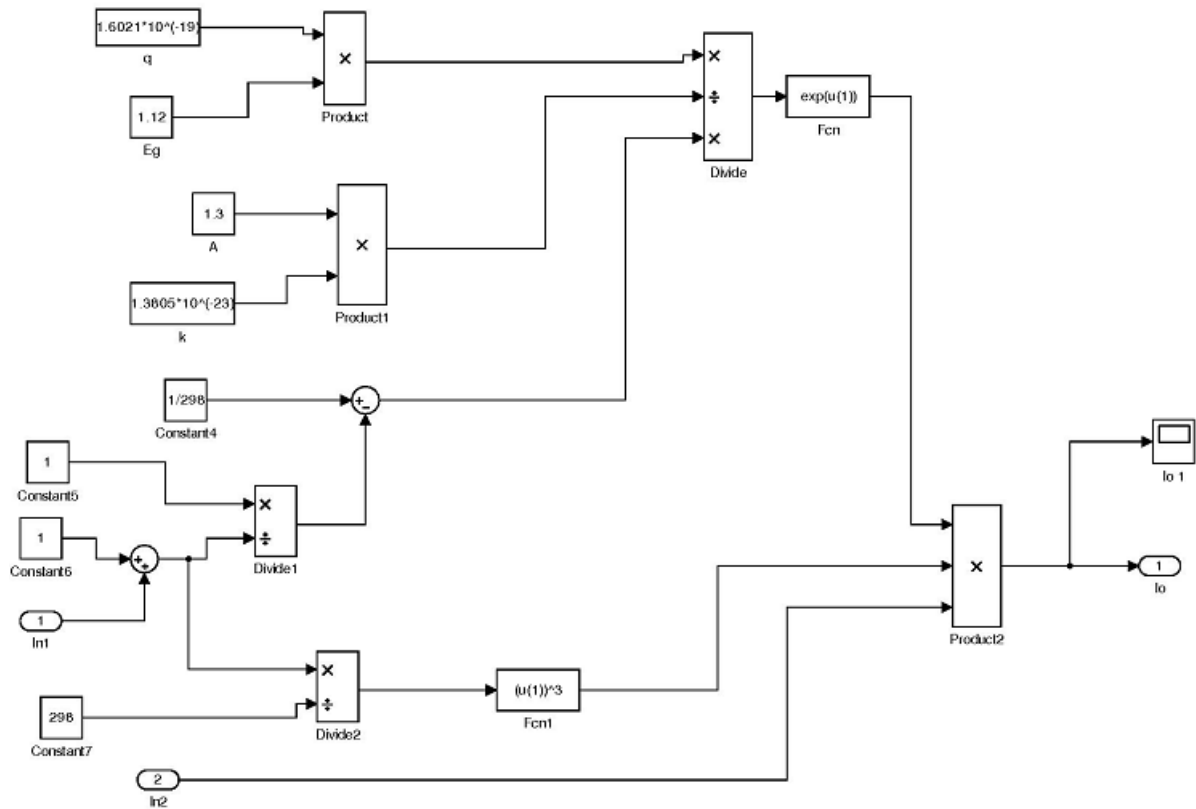


Fig: 2.4 (b) Detailed Io implementation

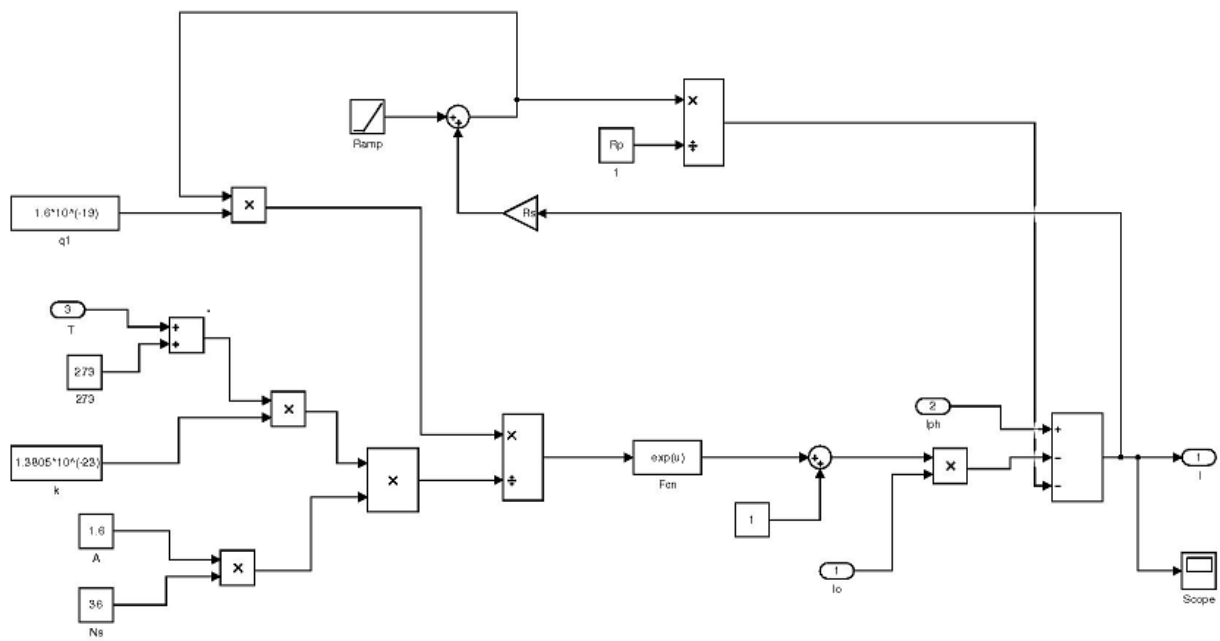


Fig: 2.4(c). Detailed model with R_p

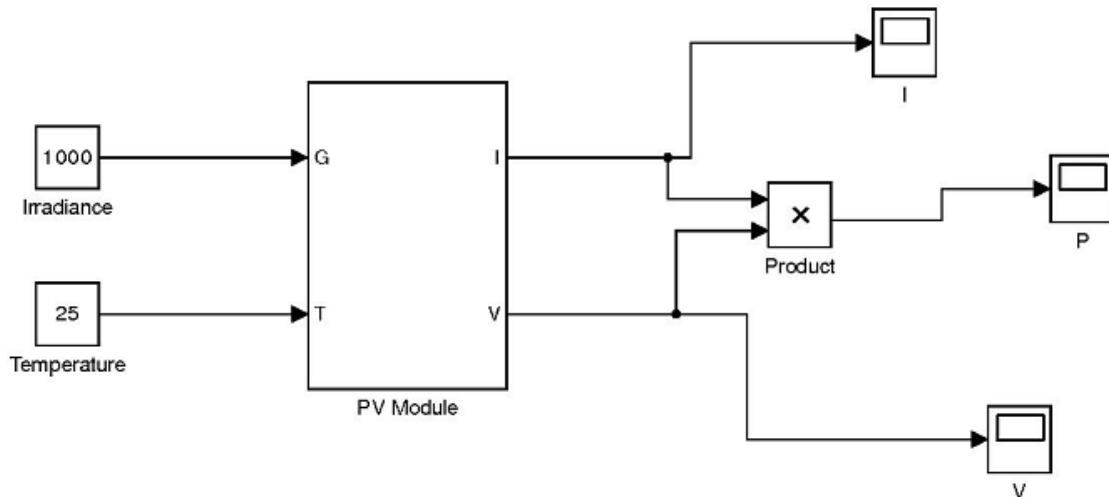


Fig: 2.4(d) The PV array model

2.5 Validation of the Model

To validate the model SunPower SPR-305 PV module was simulated. Its response was compared with the datasheet information provided by the manufacturer. The experimental value extracted from the datasheet is summarized in Table 2.1. In the table it shows the characteristics of the SPR-305 at 25⁰C. Both relevant plots: Current vs Voltage and Power vs Voltage were computed for different values of irradiance and temperature.

Table. 2.1. Datasheet parameters for SunPower SPR-305

Irradiance (W/m ²)	1000
Maximum Power (W)	305 W
Voltage at Maximum Power (V _{mp}) (V)	54.7 V
Current at Maximum Power (I _{mp}) (A)	5.58 A
Open Circuit Voltage (V _{OC}) (V)	64.2 V
Short Circuit Current (I _{SC}) (I)	5.96 A
Temperature Co-efficient of V _{OC} (K _v) (V/ ⁰ C)	-0.177
Temperature Co-efficient of I _{SC} (K _i) (A/ ⁰ C)	0.003516
No. cells in series (N _s)	5

The simulation was repeated for three different temperature values at (25-75)⁰C and for irradiance varying from 250 W/m² to 1000 W/m².

2.5.1 Current vs Voltage characteristics of a PV module

Fig 2.5.1 (a) shows the current voltage characteristics of a PV panel. It is a nonlinear curve. It shows that the maximum current is 5.58 A and maximum voltage is 54.7 V. Fig 2.5.1 (b) shows the IV curve for different values of irradiance.

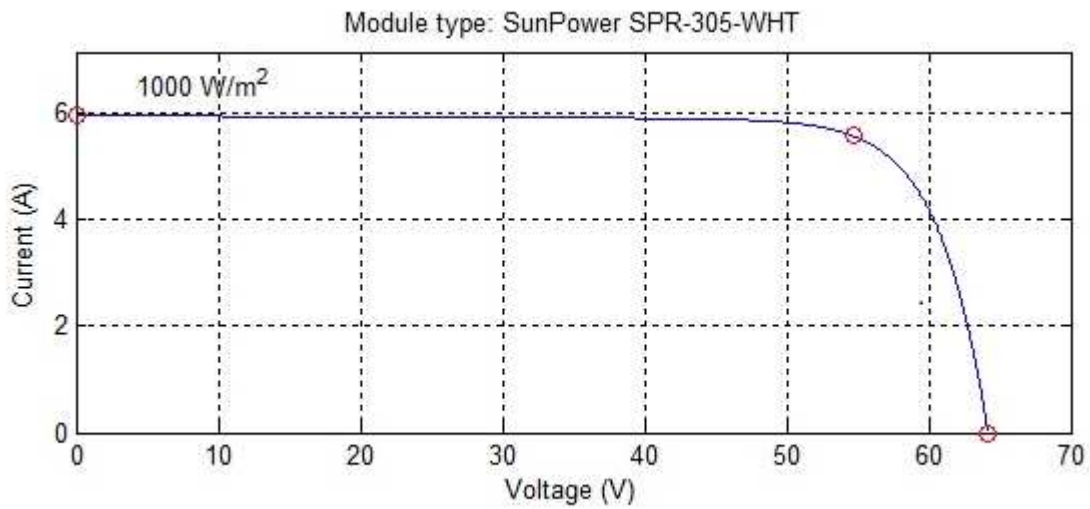


Fig. 2.5.1 (a) IV curve of PV module SunPower SPR-305-WHT

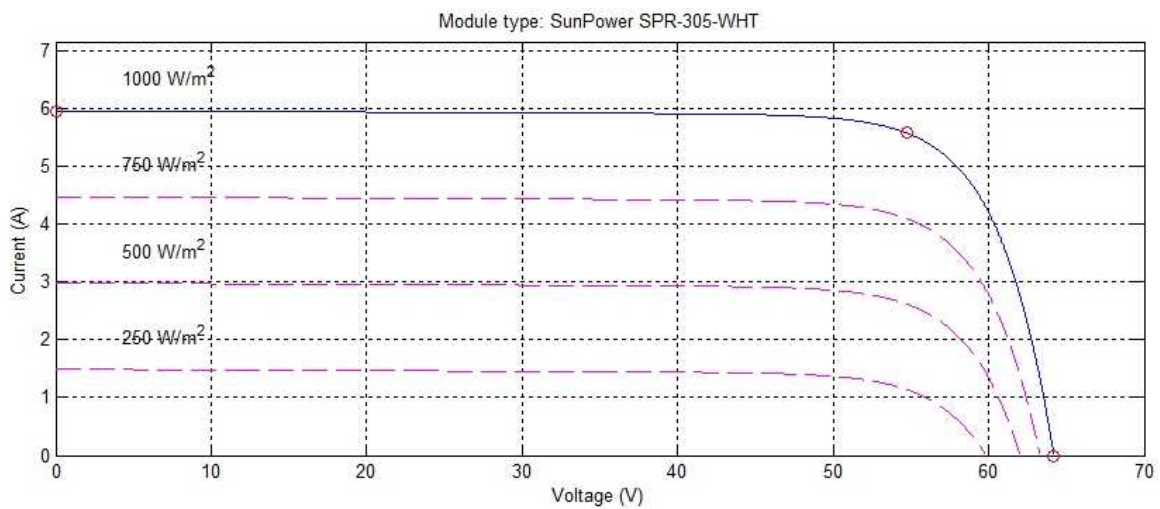


Fig 2.5.1 (b) IV curve for different values of irradiance.

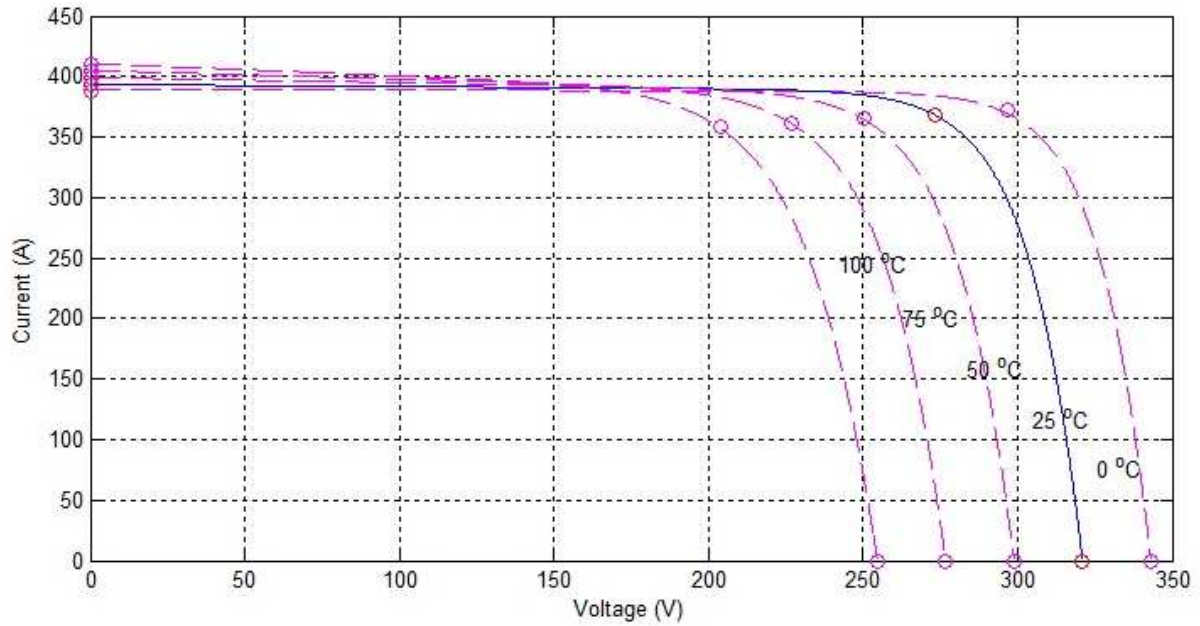


Fig: 2.5.1 (c) IV curve for different values of temperature. SunPower SPR-305-WHT 5 series modules, 66 parallel strings

2.5.2 Power vs Voltage characteristics of a PV module

Fig 2.5.2 (a) shows the Power vs Voltage characteristics of the SunPower SPR-305-WHT module. The maximum power of a single module is 305 W. Fig 2.5.2 (b) shows the variation of power with different values of irradiance.

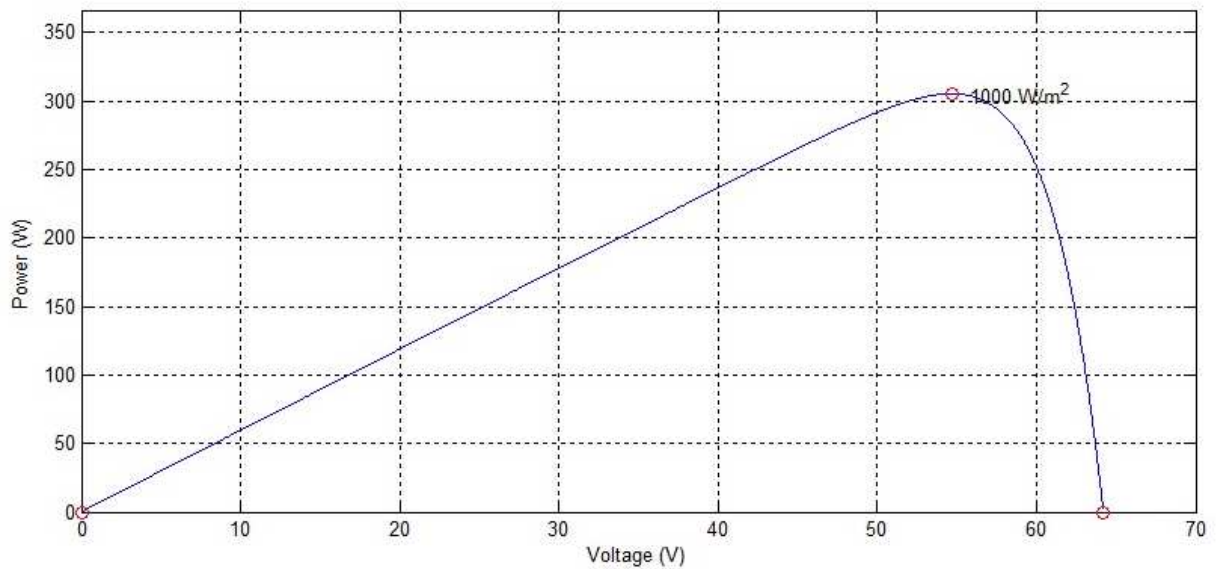


Fig: 2.5.2 (a) PV curve for module SunPower SPR-305-WHT

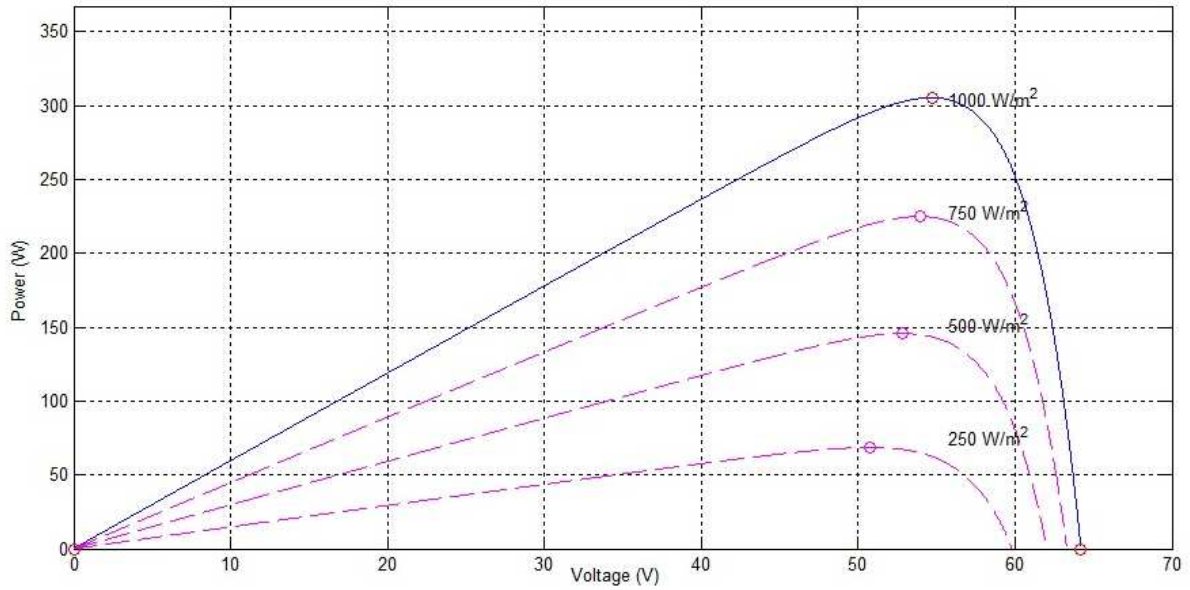


Fig: 2.5.2 (b) PV curves with different values of irradiance.

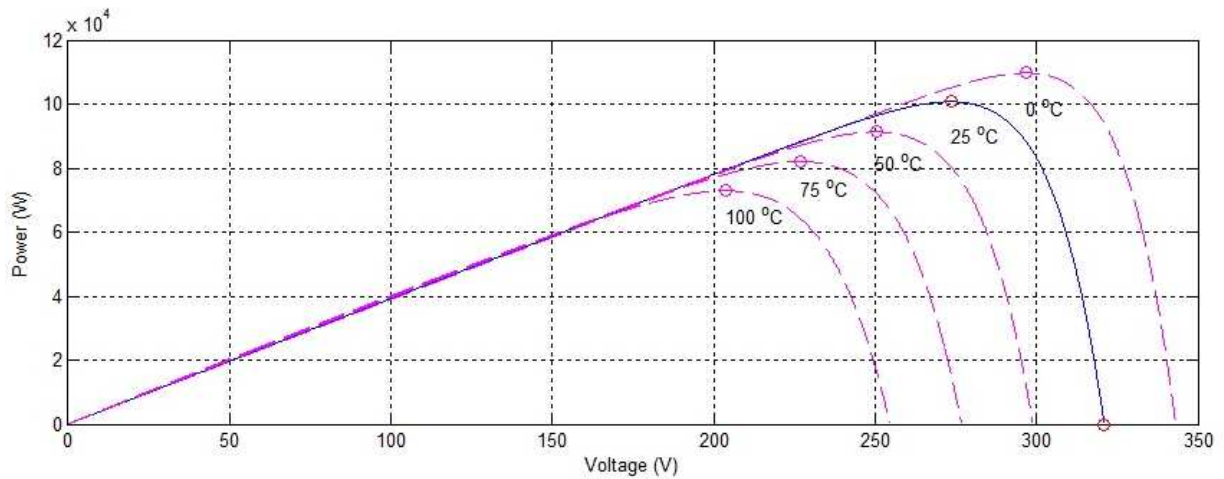


Fig: 2.5.2 (c) PV curve with different values of temperature of PV array. SunPower SPR-305-WHT 5 series modules, 66 parallel strings

Fig 2.5.1 (c) and Fig. 2.5.2 (c) shows the IV curve and PV curve of SunPower SPR-305-WHT array with 5 numbers of series connected strings and 66 parallel connected strings with different values of temperatures and sun irradiance of 1000 W/m^2 .

Table 2.2 Characteristics for 100 kW Photovoltaic Array at sun irradiance 1000 W/m^2

Number of Series connected modules (N_s)	5
Number of Modules in Parallel (N_p)	66
Maximum Output Voltage at MPP (V_{mp})	273 V
Maximum Power Output at MPP (P_{mp})	100 kW

Fig. 2.5.3(a) and (b) show the IV curve and PV curve of the SunPower SPR-305-WHT array at standard test conditions i.e, irradiance of 1000 W/m^2 and temperature of 25° C .

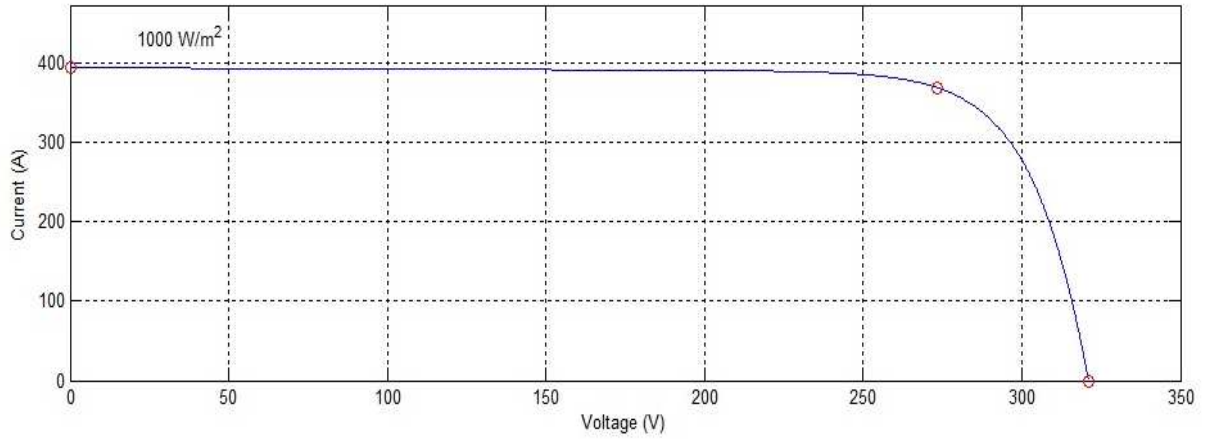


Fig: 2.5.3 (a) IV curve of SunPower SPR-305-WHT array

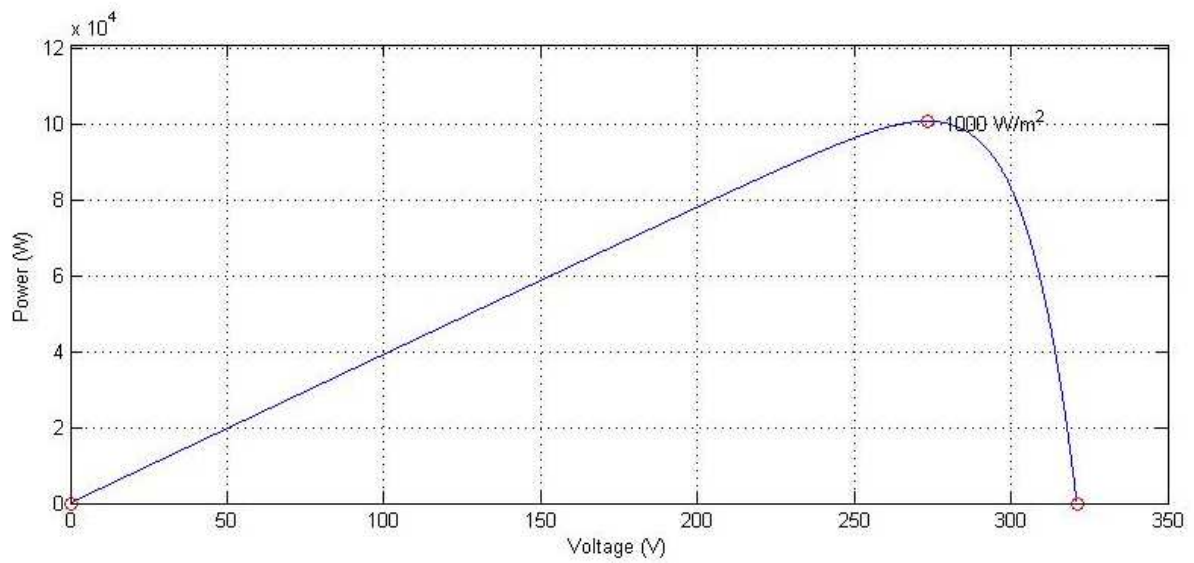


Fig: 2.5.3 (b) PV curve of SunPower SPR-305-WHT array

CHAPTER 3

MAXIMUM POWER POINT TRACKING (MPPT)

The output power of the PV module changes with variation of sun irradiance and ambient temperature. In the previous chapter the nonlinear response characteristic of the PV module could be observed. There is a single maxima point of the power vs voltage curve that corresponds to a specific voltage and current. As we know that the efficiency of a solar cell is around 8-15% [31], it is desirable to operate the module at the peak power point so that the maximum power can be delivered to the load under different environmental condition, i.e. varying temperature and irradiation levels.

The location of the maximum power point (MPP) is not known but needs to be located. Many MPPT methods have been developed and implemented for research and commercial purposes. The methods vary in complexity, cost, implementation hardware, sensors required, convergence speed and range of effectiveness [33].

3.1 MPPT Algorithm

MPPT algorithms are based on measurement of the PV module output voltage and current. This algorithm calculates the PV power and defines if the control parameter needs to be increased or decreased. This control parameter is generally a duty ratio for the switching signal of a DC/DC converter, or it could be a reference signal for a controller.

3.1.1 Model based Algorithm

MPPT with Fractional open-circuit voltage method

This method uses the approximately linear relationship between MPP voltage (V_{mp}) and open circuit voltage (V_{OC}) of the PV array under different irradiation and temperature [33].

$$V_{mp} \approx k_1 V_{OC} \tag{3.1}$$

where k_1 is a constant of proportionality and it is dependent on the characteristics of the PV array. The value of k_1 is in between 0.71 to 0.78. It has to be determined beforehand for determining V_{mp} for the specified PV array at the different values of irradiance and temperature.

MPPT with Fractional short-circuit current method

As in the previous method, here also there is a relationship between MPP current (I_{mp}) and short circuit current (I_{SC}) of the PV array under different irradiance and temperature levels.

$$I_{mp} \approx k_2 I_{SC} \quad 3.2$$

Here k_2 is constant of proportionality, and it has to be determined according to each PV array, as was with k_1 in the previous method. The value of the constant is in between 0.78 to 0.92 [33].

Both methods are easy to implement and cheap, but there is excessive power loss and the efficiency of the PV panel is very low due to inaccurate determination of the constant k_1 and k_2 .

Among various MPPT methods used the two most widely used methods are Incremental Conductance (INC) method and Perturbation and Observation (P&O) methods.

3.2 Perturbation and Observation (P&O) Method

This is one of the most conventional methods of MPPT algorithm. As the name implies this method will perturb the system by increasing or decreasing the output terminal voltage of the PV array and compare the result with value obtained in the previous perturbation cycle. If the perturbation leads to an increase or decrease in the output array power, then the subsequent perturbation is made in the same or opposite direction. In this way the power tracker continuously finds the peak power condition. In this algorithm the voltage V is constantly perturbed with every step calculation meaning V will oscillate around the ideal voltage V_{mp} . To keep small power variation the perturbation size is also kept small, which leads to an obvious drawback as the time required to reach the peak power point is large. If the variation is large, then the oscillation around the V_{mp} will be larger, causing power loss.

The value of the optimal step size is unique to every system. The starting value of duty cycle is set at 50%. The process is repeated until the MPP is reached. So the system oscillates around the MPP. This problem can be minimized by reducing the perturbation step size [33]. Fig. 3.1 explains the flow chart of perturb & observe method. Photovoltaic voltage and current are the input and output power is calculated from these two parameters. The sign of the output power determines the duty cycle output of the MPP controller. Duty ratio of the boost converter is the control variable. Perturbing the duty ratio of the converter perturbs the PV array current and consequently perturbs the PV array voltage.

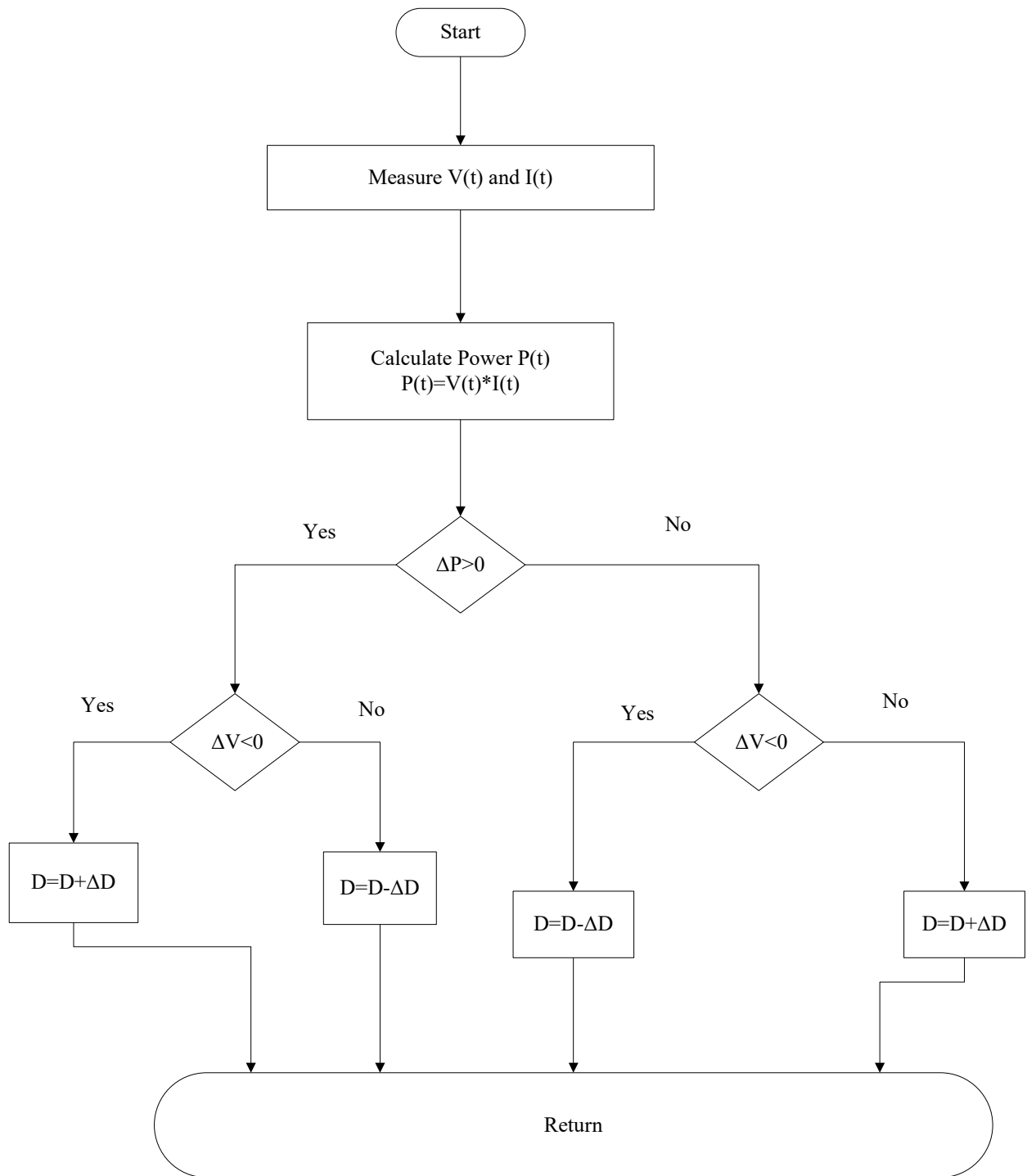


Fig: 3.1 Flow chart of P& O method.

This is a complete flowchart of P & O method for one complete cycle. The computational steps are as follows:

- Step 1: Measure the voltage and current, from the output of PV array and calculate the power from it.
- Step 2: Compare the calculated power with the power obtained in the last perturbation cycle.
- Step 3: Check the nature of change in power and also the change in corresponding voltage.
- Step 4: Control the voltage change by changing the duty ratio.
- Step 5: Return the value.

3.1.3 Incremental Conductance Method

The incremental conductance method seeks to overcome the limitations of the Perturb & Observe method. This algorithm uses the condition that the derivative of power with respect to voltage at the maximum power point is zero. In this method the current changes with the change in irradiance and temperature. In the incremental conductance method the PV model operates at maximum power when the reference voltage is reached. The algorithm tracks the new MPP with varying the duty cycle.

The equations written below are describes the incremental conductance algorithm

$$P = V * I \tag{3.1}$$

Deriving both sides with respect to V, we have:

$$\frac{dP}{dV} = \frac{d(V.I)}{dV}$$

$$\frac{dP}{dV} = V * \left(\frac{dI}{dV} \right) + I * \left(\frac{dV}{dV} \right)$$

$$\frac{dP}{dV} = I + V * \left(\frac{dI}{dV} \right) \tag{3.2}$$

Since, it is known that

$$\frac{dP}{dV} = 0 \tag{3.3}$$

Now it can be written as:

$$\frac{dI}{dV} = -\frac{I}{V} \quad \text{At MPP} \quad 3.4$$

$$\frac{dI}{dV} > -\frac{I}{V}; \text{ left of MPP} \quad 3.4.a$$

$$\frac{dI}{dV} < -\frac{I}{V}; \text{ right of MPP} \quad 3.4.b$$

From equation 3.4 it can be written that

$$\frac{dI}{dV} + \frac{I}{V} = 0 \quad 3.5$$

Here equation (3.5) is used and its output is fed to an integral regulator which corrects the duty cycle. The incremental regulator minimizes the error $\left(\frac{dI}{dV} + \frac{I}{V}\right)$. The duty cycle is varied and this variation varies the boost converter voltage. The PV array will operate at maximum power with the duty cycle controlled through MPPT controller.

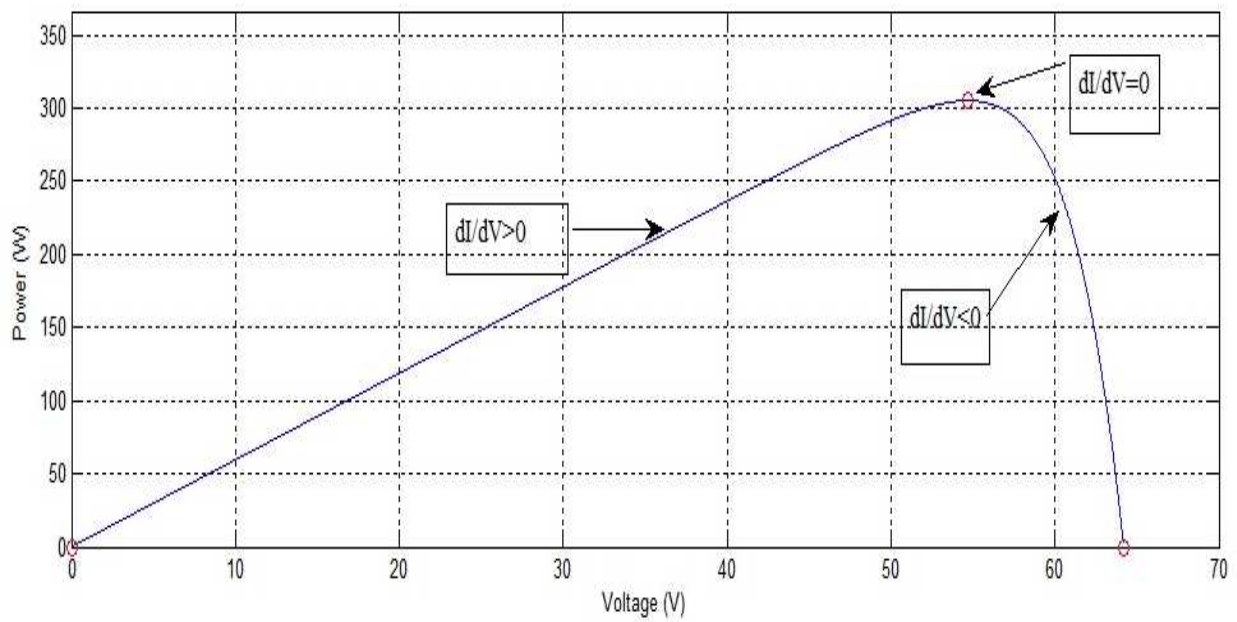


Fig: 3.2 PV curve of SunPower SPR-305-WHT

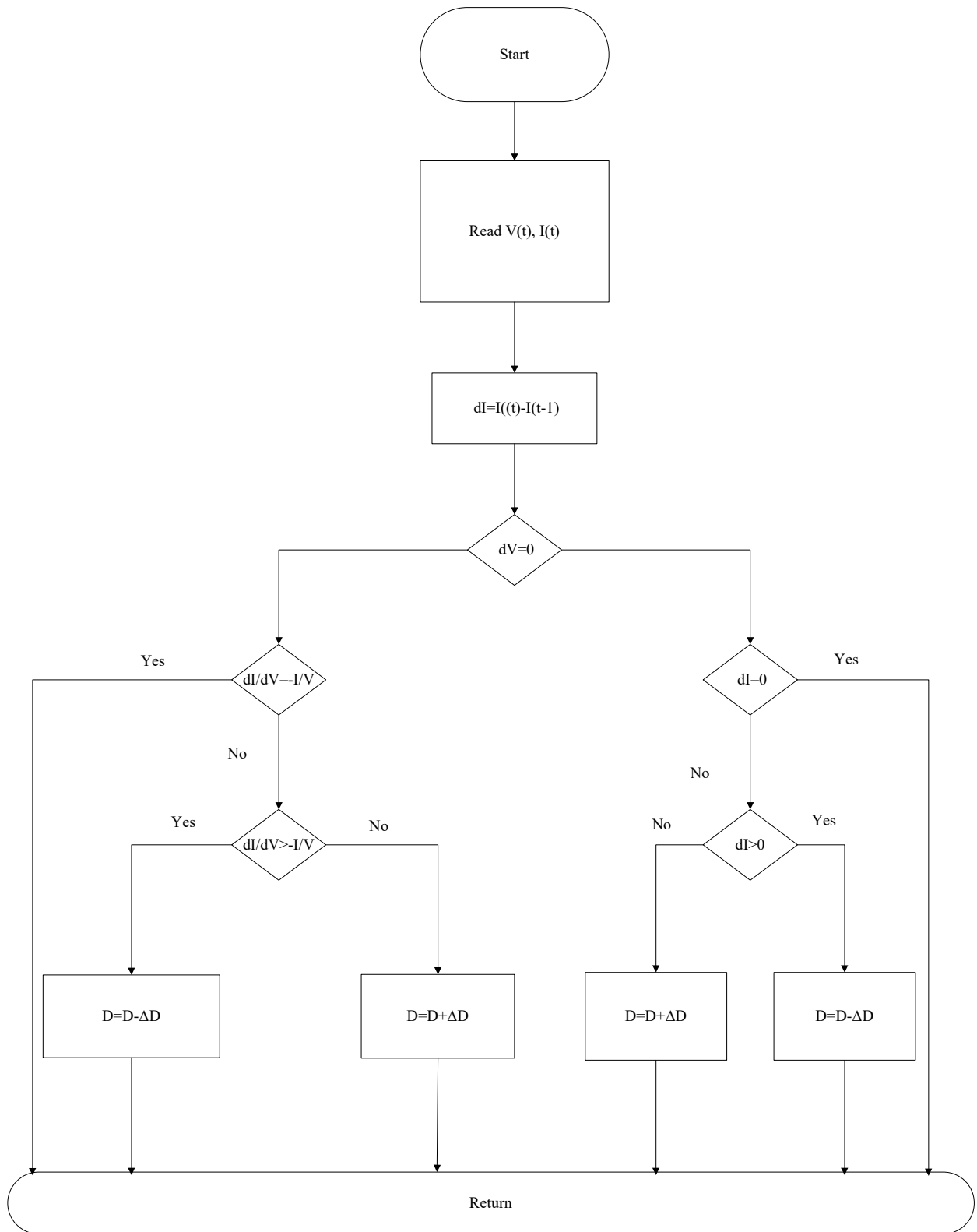


Fig: 3.3 Flow chart of Incremental Conductance Algorithm

This is the flowchart of INC method. The computational steps are as follows.

- Step 1: Measure the voltage and current from the PV array and calculate the power
- Step 2: First calculate the change in current. Then check the voltage change.
- Step 3: If there is no voltage change then verify the current, if there is no change then go to step 7
- Step 4: If there is a change in current, then verify whether it is increasing or decreasing, if increasing then reduce the duty ratio, and if it is decreasing then increase the duty ratio and go to step 7
- Step 5: If there is some change in voltage then check the change in current with respect to voltage and compare it with the ratio of current to voltage. If it is equal to the I/V ratio then go to step 7
- Step 6: If the dI/dV is increasing to I/V then reduce the duty ratio and to go to step 7, if dI/dV is decreasing to I/V then increase the duty ratio and go to step 7
- Step 7: Return the value.

For the purpose of the thesis work the SIMULINK representation of this INC MPPT method is shown and discussed in Chapter 6.

CHAPTER 4

DC-DC BOOST CONVERTER

The PV array produces DC voltage at its output terminal. The DC-DC converter converts the output voltage from PV array into a higher value of DC voltage. The maximum power point tracker controls the DC-DC converter to track the voltage at the maximum power point.

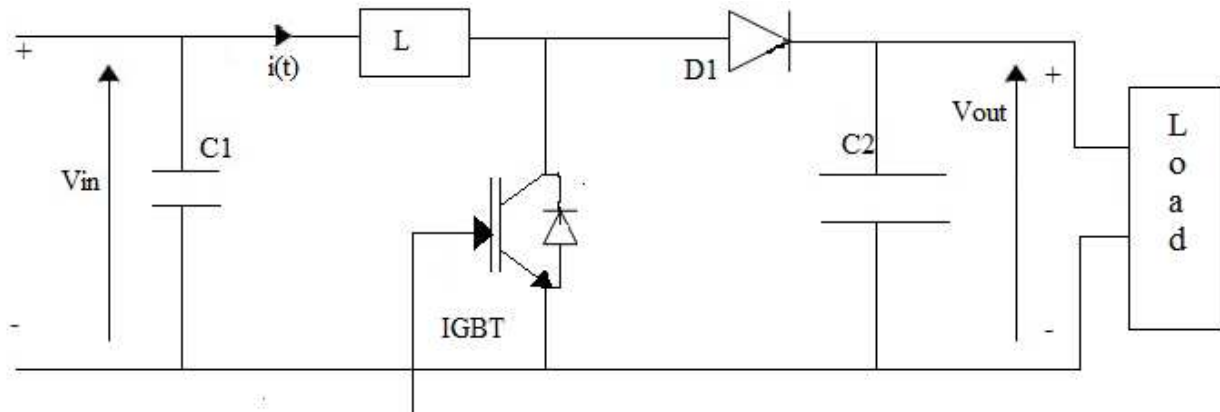


Fig: 4.1 DC-DC Boost Converter

The above figure shows the boost converter. The DC input is in series with an inductor L which acts as a current source. IGBT is in parallel with the current source and is switched on and off periodically. The voltage ratio for a boost converter is the time integral of the inductor voltage over a switching period to zero [24]. The voltage ratio of the converter can be written as:

$$\frac{V_0}{V_i} = \frac{T_s}{t_{off}} = \frac{1}{1-D} \quad 4.1$$

Where,

- V_i = Input voltage V
- V_0 = Output voltage
- t_{off} = Off time of the IGBT
- T_s = Switching period
- D = The duty cycle

The value of the capacitor C_2 at the output terminal is chosen to be large to keep a constant output voltage, and when the switch is open the inductor supplies energy boosting the voltage

across the load. The MPPT controller controls the switching device through the duty cycle. It is a gate signal that turns on and off the device by pulse width modulation.

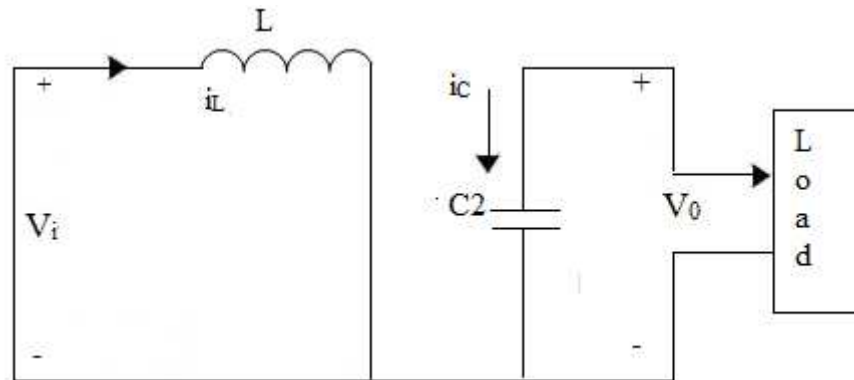


Fig: 4.1 (a) IGBT is ON and diode D1 is OFF

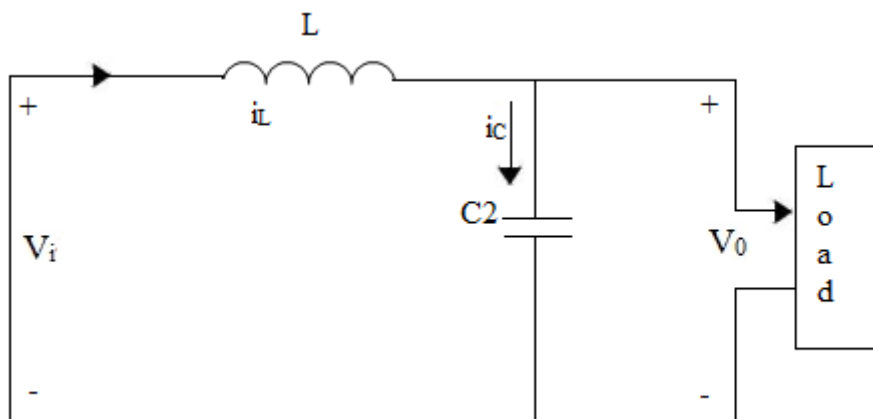


Fig: 4.1 (b) IGBT is OFF and diode D1 is ON

In Fig. 4.1(a) IGBT is on and diode D_1 is off, whereas in Fig. 4.1(b) the IGBT is off and diode D_1 is on. In this mode, the energy is stored in the inductor along with DC supply. This will help to supplement power for the circuit resulting in a boost for the output voltage.

$$v_L = V_i ; \text{ When IGBT is on}$$

$$v_L = V_i - V_0 \text{ when IGBT is off and diode } D_1 \text{ is ON}$$

Under stabilized condition the integral of the inductor voltage over the time period T_s has to be zero

So,

$$\int_0^{T_s} v_L(t) dt = (V_i)DT_s + (V_i - V_0)(1-D)T_s$$

If we equate this to zero, we get

$$V_0 = \frac{V_i}{1-D}$$

Since ($P_i = P_0$)

$$\frac{I_0}{I_i} = 1-D$$

From the above relationship it can be stated that the output voltage is proportional to the duty cycle D . The output voltage increases as D increases. Thus the boost converter can produce the output voltage higher than the input voltage.

This converter can operate in two different modes - continuous conduction mode (CCM) and discontinuous conduction mode (DCM).

4.1 Continuous Conduction Mode (CCM):

In the CCM mode the IGBT switched on for a period t_{on} as shown in figure 4.2. The inductor current is positive and ramp up linearly and the inductor voltage is V_i . The inductor current decrease until the IGBT is turned on again during the next cycle. The voltage across the inductor is the difference between V_i and V_0 .

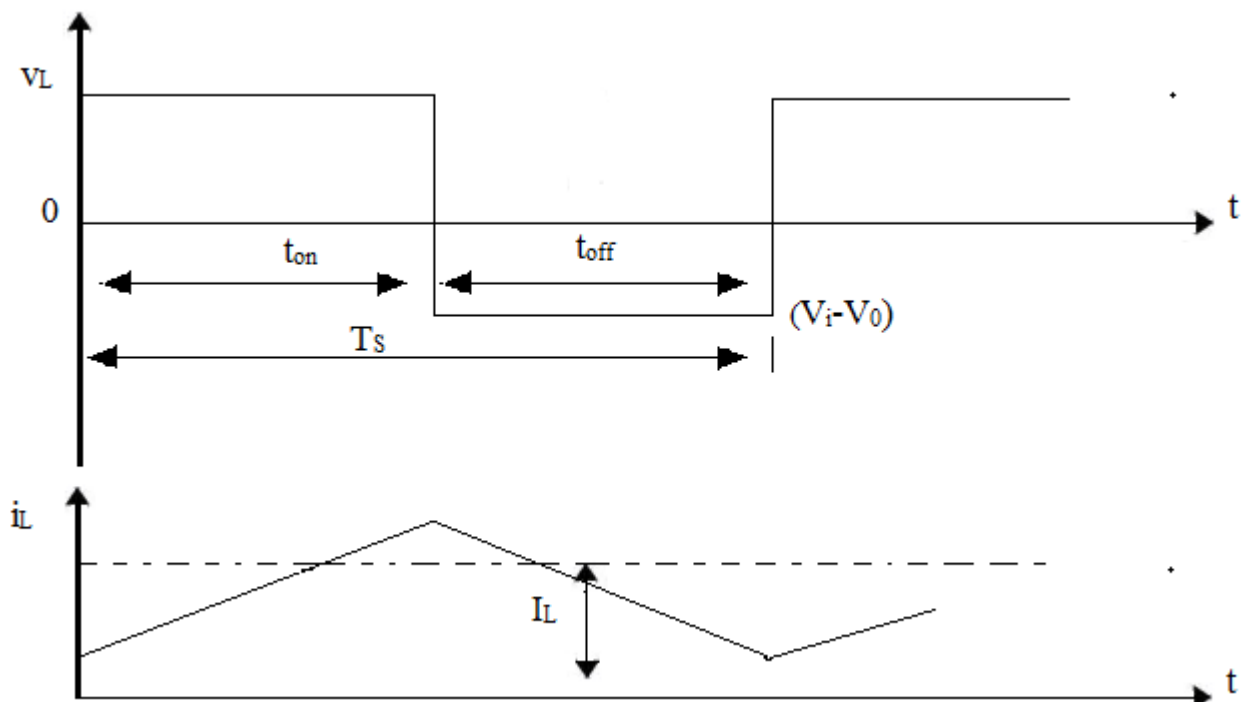


Fig: 4.2 Continuous Conduction Mode [24]

4.2 Discontinuous Conduction Mode (DCM):

If the current flowing through the inductor falls to zero before the next turn-on of the switching IGBT, then the boost converter is said to be operating in the discontinuous conduction mode.

The relation between the input and output voltage become

$$\frac{V_0}{V_i} = \frac{D_1 + D}{D_1}$$

The average input current which is equal to the inductor current is [24]

$$I_i = \frac{V_i}{2L} DT_s (D + D_1)$$

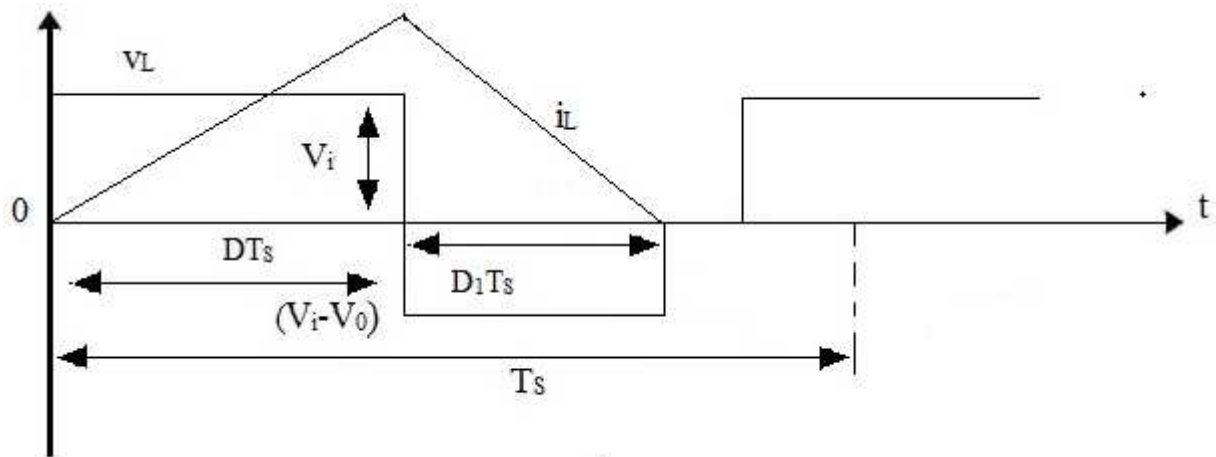


Fig: 4.3 Discontinuous Conduction Mode [24]

Figure 4.4 briefly explains the output current and output voltage of the boost converter. The control voltage for IGBT is shown. The switch turns ON and OFF for a period of t_{on} and t_{off} . When the switch is on, the voltage across the switch is zero and once the switch is turned off, the voltage is V_0 . The voltage across the inductor L is equal to the photovoltaic voltage during the on time of the transistor.

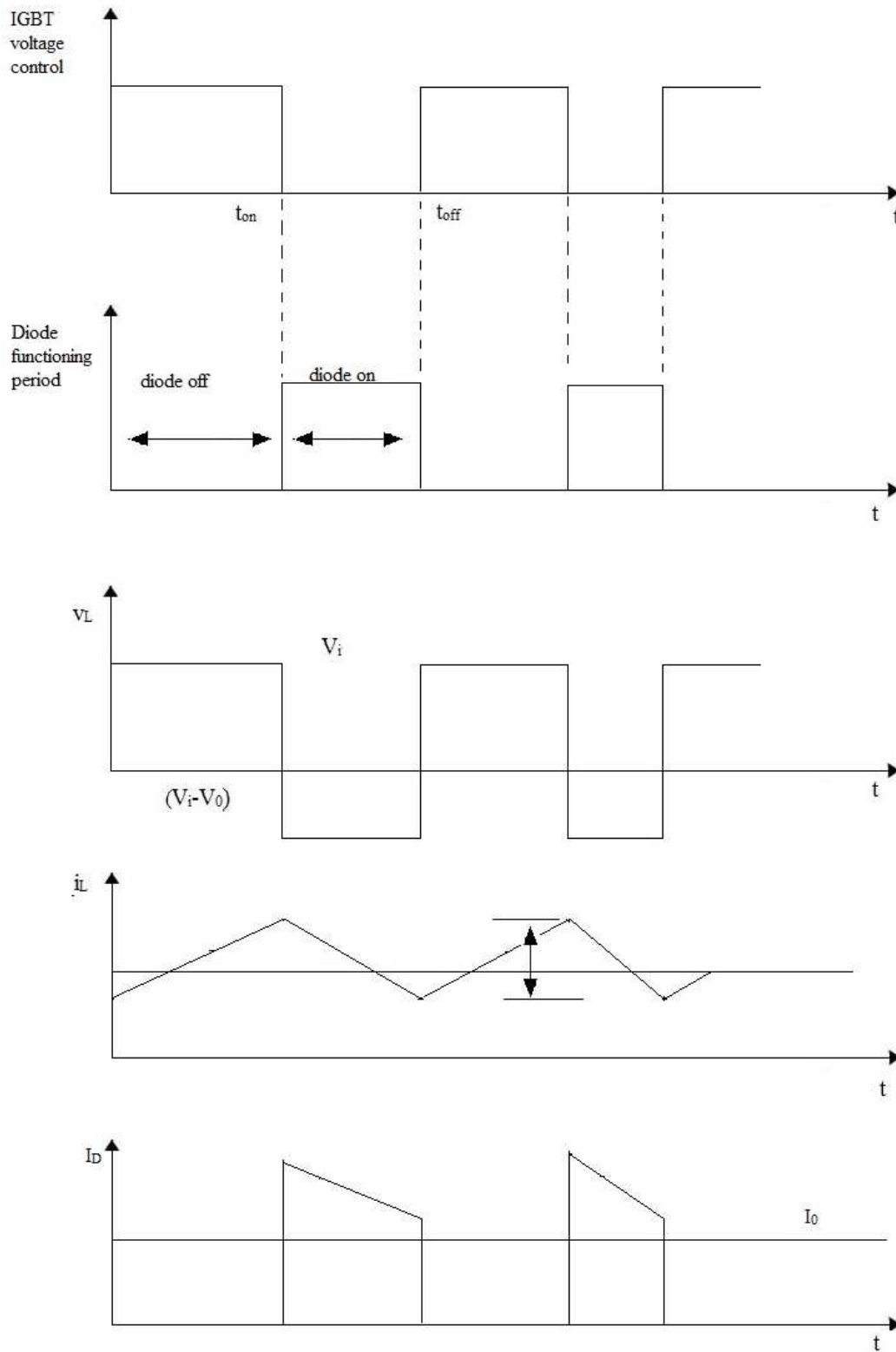


Fig: 4.4

CHAPTER 5

INVERTER TOPOLOGY

The main purpose of the inverter is to convert the DC voltage obtained from DC-DC converter into a symmetrical ac output voltage of desired magnitude and frequency. By varying the gain of the inverter a variable output voltage can be obtained, which is accomplished by pulse width modulation (PWM) control within the inverter. The gain of the inverter may be defined by the ratio of the ac output voltage to dc input voltage. For higher power application three-phase inverters are normally used. Three single-phase inverters can be connected in parallel as shown in Fig 5.1

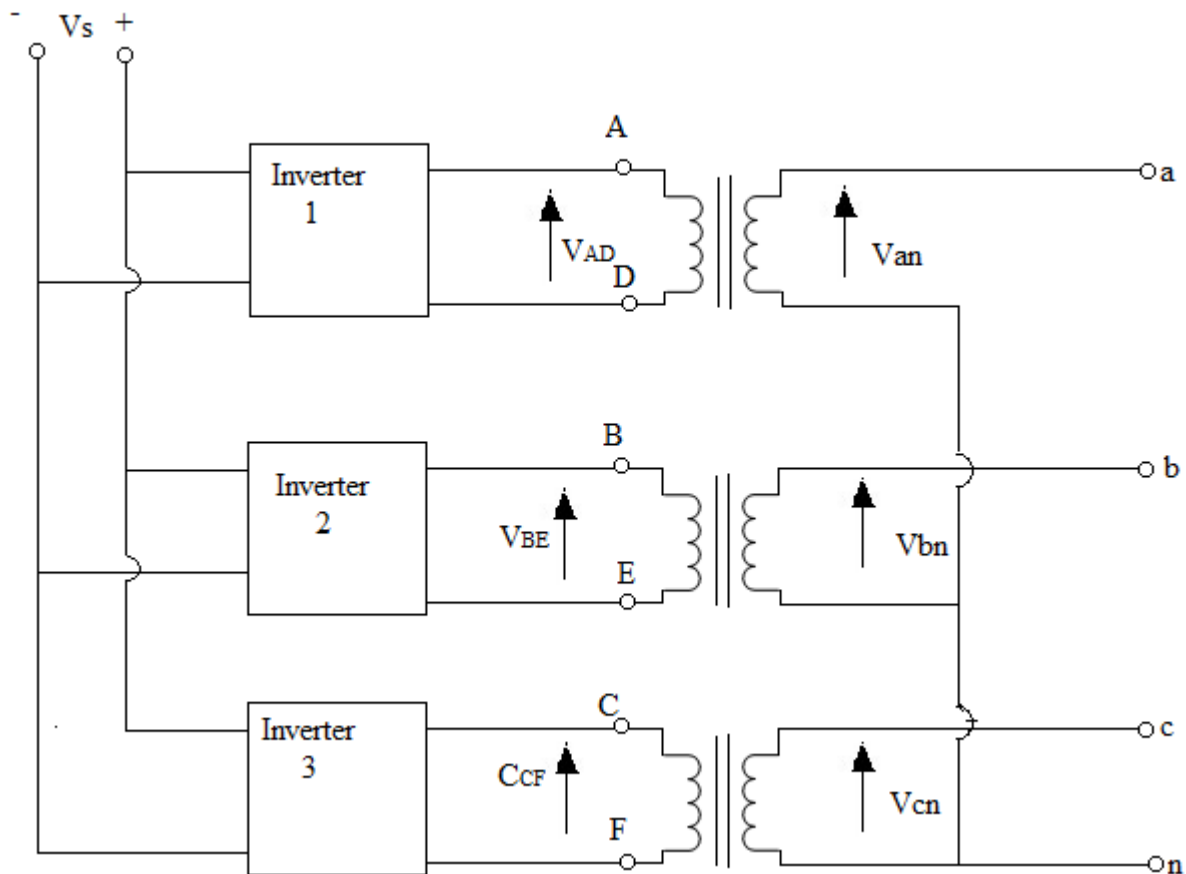


Fig: 5.1 Three phase inverter

Power electronic inverter is often known as power conditioning unit. It connects the utility grid with the PV source. Selection of a proper power electronic arrangement reduces the number of stages in the system, which makes the whole system more economical. Reference

[35] provides a survey on the structure of power electronic interface used in three-phase grid connected PV systems on how the boost converter is controlled. After thorough investigation of various inverters, VSI has been found to be the most suitable for integrating PV arrays into the utility grid. Fig 5.2 (a) gives a schematic diagram of VSI topology connected to three phase grid.

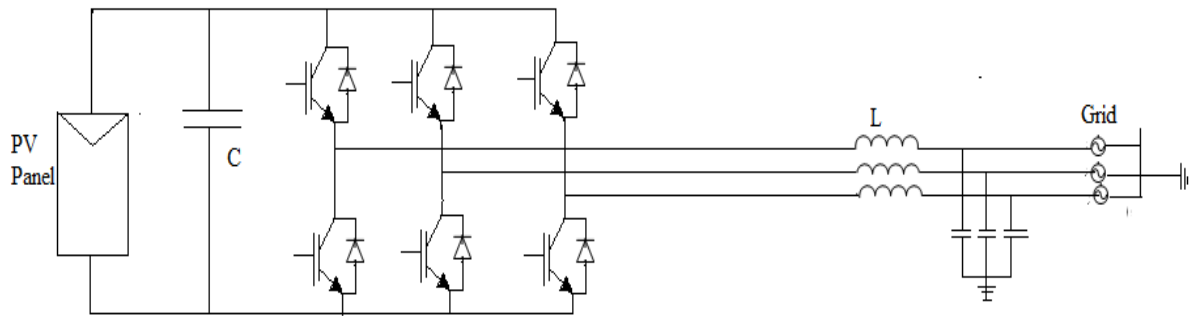


Fig: 5.2 (a) Voltage Source Inverter

VSI topology provides a simple and effective control technique and well established Pulse Width Modulation techniques. One major drawback of VSI is the buck topology. VSI requires sufficiently high voltage for proper functioning. Therefore boost converter is employed between the DC source and VSI during low input voltage. Fig 5.2 (b) shows the connection between the VSI and a boost converter. On the other hand, the topology that has been less investigated and adopted when compared with VSI for grid-interface application is Current Source Inverter (CSI) topology. Fig 3.2 (c) shows the schematic diagram of CSI. Recently a new topology named “Impedance-Inverter” or Z-source inverter has been adopted for interfacing distributed generation. The special feature of this type of inverter is that it overcomes the limitations of the traditional VSI and CSI scheme and it can capable to perform the operations in both buck and boost modes. Applications of Z-source inverter in the grid connected PV system is at a very early stage. Since this type of inverter is capable of operating in both buck and boost mode, a comparative study between buck boost inverter and Z-source for PV application is carried out in [36]. In [36] it is shown that the efficiency of Z-source inverter drops more rapidly for high loads compared to that of buck-boost converter. Though the Z-source inverter can operate both in step up and step down mode it brings more complexity compared with single stage grid connected PV system based on VSI or CSI.

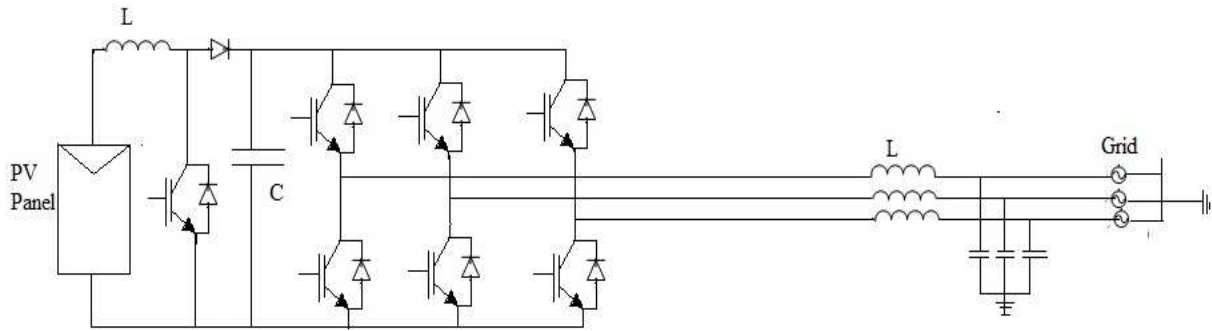


Fig: 3.2 (b) Voltage Source Inverter with a boost converter

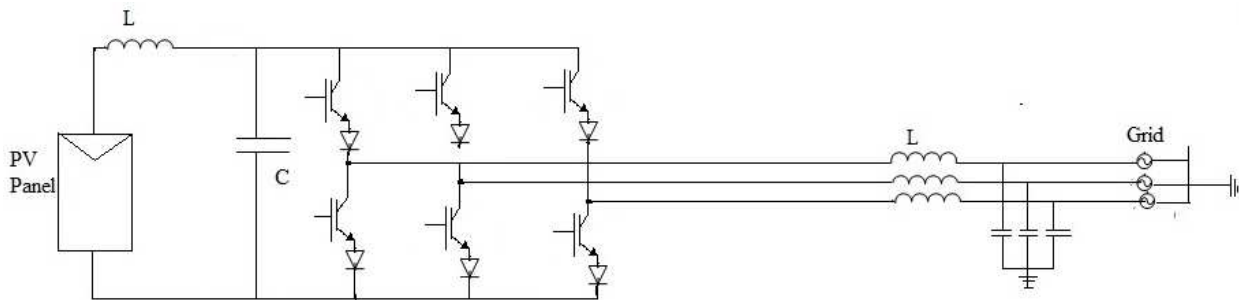


Fig: 5.2 (c) Current Source Inverter

Due to lower efficiency CSI scheme lags behind that on VSI in DG application. High energy losses in DC-link inverter and less investigated appropriate PWM switching strategies are its drawback. Recent developments in RB-IGBT (Reverse blocking Insulated Gate Bipolar Junction Transistor) have contributed towards reduced conduction losses in CSI. RB-IGBT is special type of IGBT whose structure is similar to conventional IGBT except for the fact that it has a collector isolation area that allows the IGBT to block reverse voltage.

5.1 Comparison between CSI and VSI scheme

The CSI topology offers so many advantages over the VSI topology from the viewpoints of short circuit current limiting, harmonics and losses. CSI offers direct controllability of the output current. Moreover CSI provides high reliability due to inherent short circuit current protection capability. The DC link reactor, which is the link between DG and inverter has longer lifetime in CSI than in VSI. As mentioned in the above a high input voltage is required for stable operation of VSI. Hence grid connected VSI may require an additional DC-DC boost converter if a transformer is not used. However VSI offers some advantages over CSI topology regarding efficiency and ease of control. The control scheme and pulse width modulation techniques for VSI topology are more established and more thoroughly investigated when compared to those for CSI. For FACTS (Flexible AC Transmission

System) application, [37] presents a systematic comparison of these two topologies VSC (Voltage Source Converter) and CSC (Current Source Converter). In [39] there is a comparison between VSC boost converter topology with a single stage CSI topology with IGBT switches. Here the analysis shows that in terms of losses IGBT based voltage source converter combined with boost converter scheme is more advantageous compared to current source inverter for fuel cell application. Owing to this advantage and more established PWM technique, for our work, VSI has been used to interface the PV array with the utility grid.

5.2 Voltage-Sourced Converter (VSC)

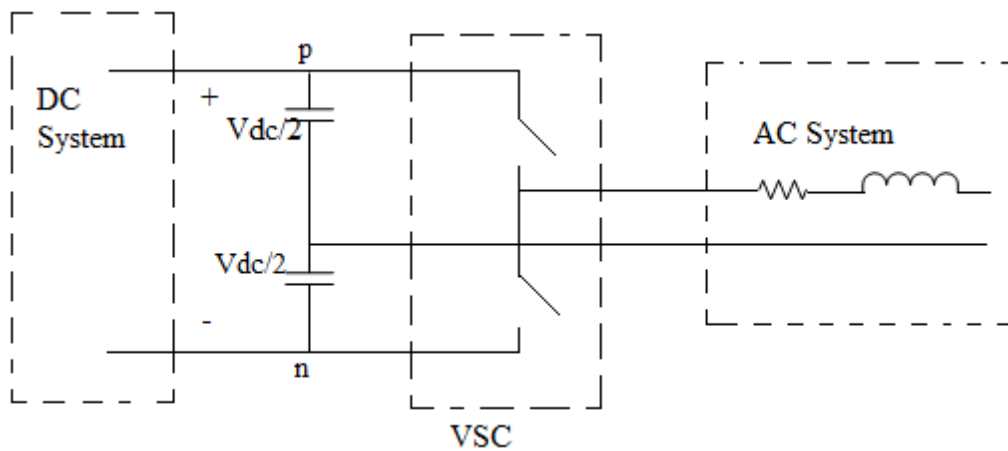


Fig: 5.3 Circuit diagram

This is the basic circuit diagram of single phase two level voltage source converter. It comprises an upper switch cell and a lower switch cell. Each switch cell is composed of a fully controllable, unidirectional switch in antiparallel connection with a diode. The DC system that maintains the net voltage of the split capacitor can be a DC source battery or a more elaborate configuration such as the DC side of the converter. The switched AC voltage at any instant is either at the voltage of p node or at the voltage of node n depending on which cell is on. The fundamental component of the AC side voltage is usually controlled based on a pulse width modulation (PWM) technique [28].

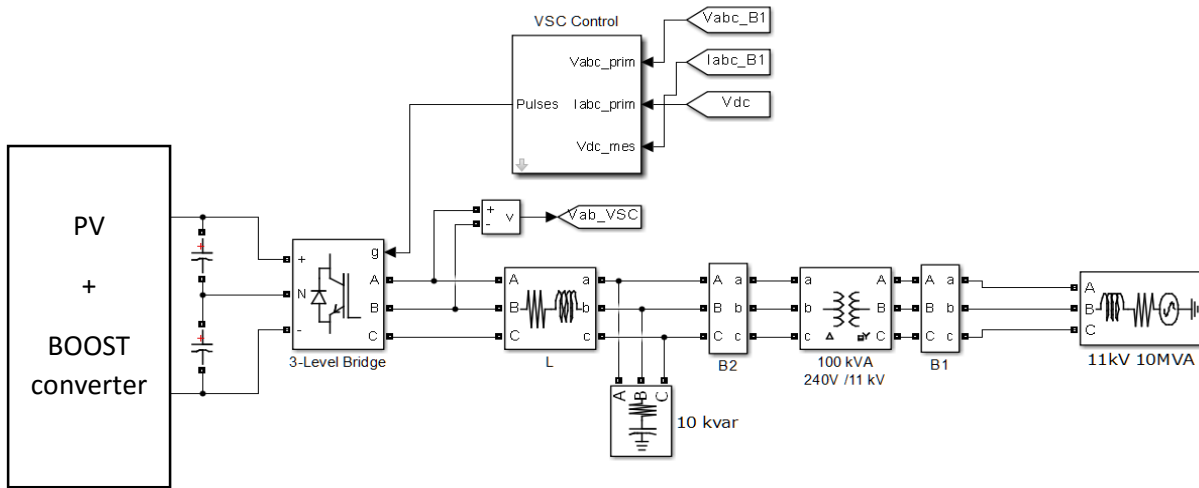


Fig: 5.4 VSC interfaced system

Fig. 5.4 above shows the Voltage source converter (VSC) interfacing the PV system with the AC grid. VSC convert the DC voltage obtained from the DC-DC converter into AC voltage. VSC is connected through two identical DC link with the boost converter. Midpoint link is chosen for voltage reference node. The connection between the AC side terminal and supply system is established through an interface reactor consisting of a series combination of resistance and inductance. The voltage at AC side of VSC is a switched waveform and contains voltage ripple. Thus the interface reactor acts as a filter and ensures a low ripple AC-side current [28].

5.3 Control of Voltage Sourced Converter

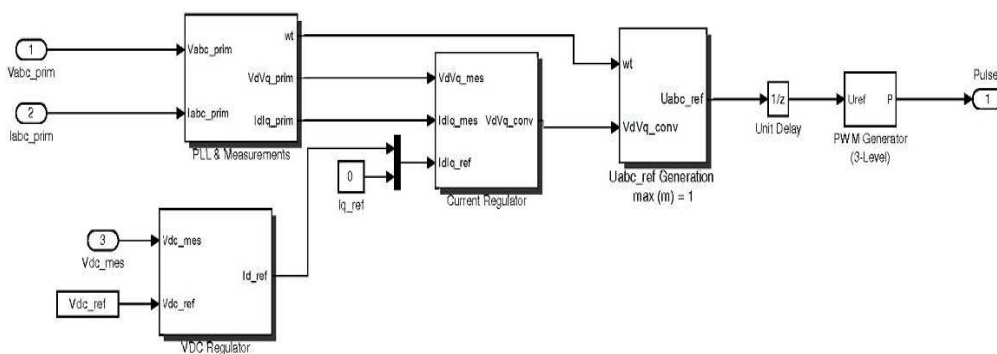


Fig: 5.5 Model of VSC Controller

Fig. 5.5 shows the detailed Simulink model of VSC controller. The VSC control system uses two control loops: an external control loop which regulates DC link voltage and an internal control loop which regulates Id and Iq grid currents. Id (active current component) current

reference is the output of the DC voltage external controller. I_q (reactive current component) current reference is set to zero in order to maintain unity power factor. V_d (active voltage component) and V_q (reactive voltage component) voltage outputs of the current controller are converted to three modulating signals U_{abc_ref} used by the PWM Generator.

Compared to the abc-control frame, the $\alpha\beta$ - control frame of a grid-imposed frequency VSC systems reduces the number of plants to be controlled from three to two. Moreover, instantaneous decoupled control of the real and reactive power, exchanged between the VSC system and the AC system is possible in $\alpha\beta$ -frame. dq - control frame of a grid imposed VSC system features all the merits of $\alpha\beta$ - frame, in addition to the advantage that the control variables are DC quantities in steady state. This feature facilitates the compensator design, especially in variable frequency schemes. In the dq - control frame, zero steady state error is readily achieved by including integral terms in the compensator since the control variables are DC quantities. Compared to the $\alpha\beta$ - control frame the dq - control frame requires a synchronizing mechanism that is usually achieved through the phase locked loop (PLL). This mechanism is used in this control scheme.

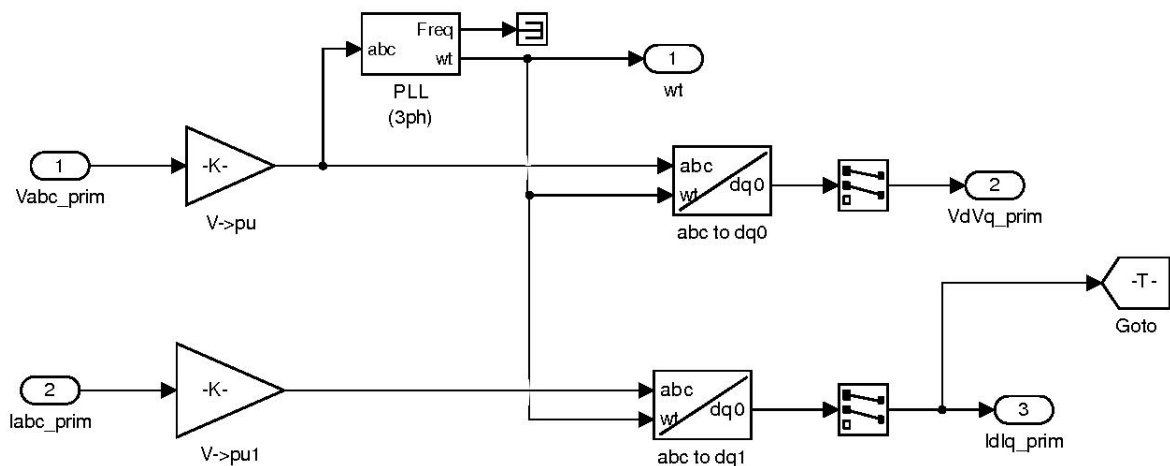


Fig: 5.6

Fig. 5.6 shows the detailed model of phase locked loop (PLL) block. This block provides a synchronization mechanism. In the dq frame, the PLL block estimated the angle of grid voltage. The real and reactive component voltage is transformed to d (real) and q (reactive) axis component

Two main methods exist for controlling active power and reactive power in the VSC system. One is voltage mode control and another is current mode control. The voltage mode control is

simple and has a low number of control loops. In the current mode control mode real and reactive power are controlled by the line current component I_d and I_q . The feedback and feed-forward signals are first transformed to the dq -frame and then processed by compensators to produce control signals in dq -frame. Finally the control signals are transformed to the abc -frame and fed into VSC.

Fig 5.7 shows the model of voltage regulator. A proportional integral (PI) compensator is used to track the reference value of current.

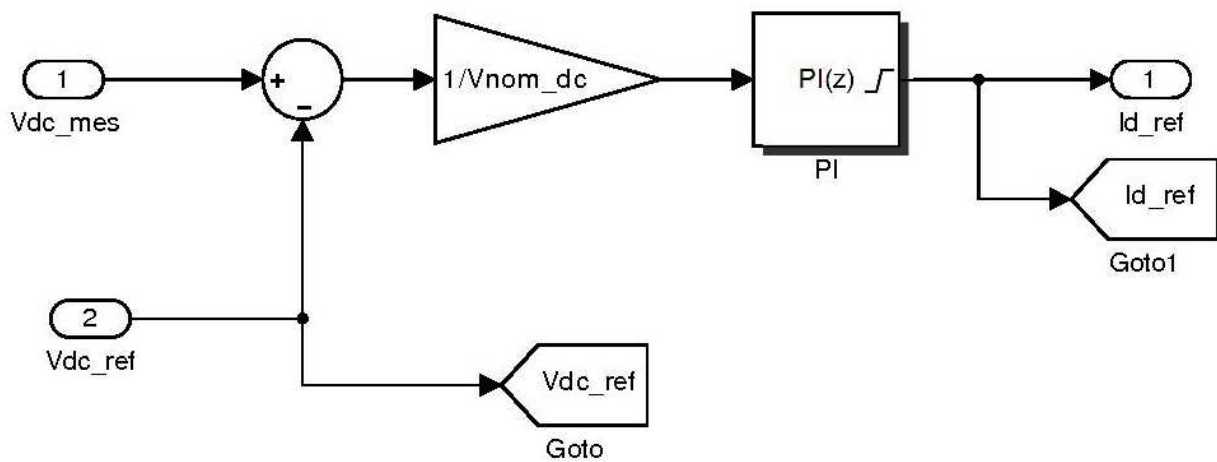


Fig: 5.7 Model of Voltage Regulator

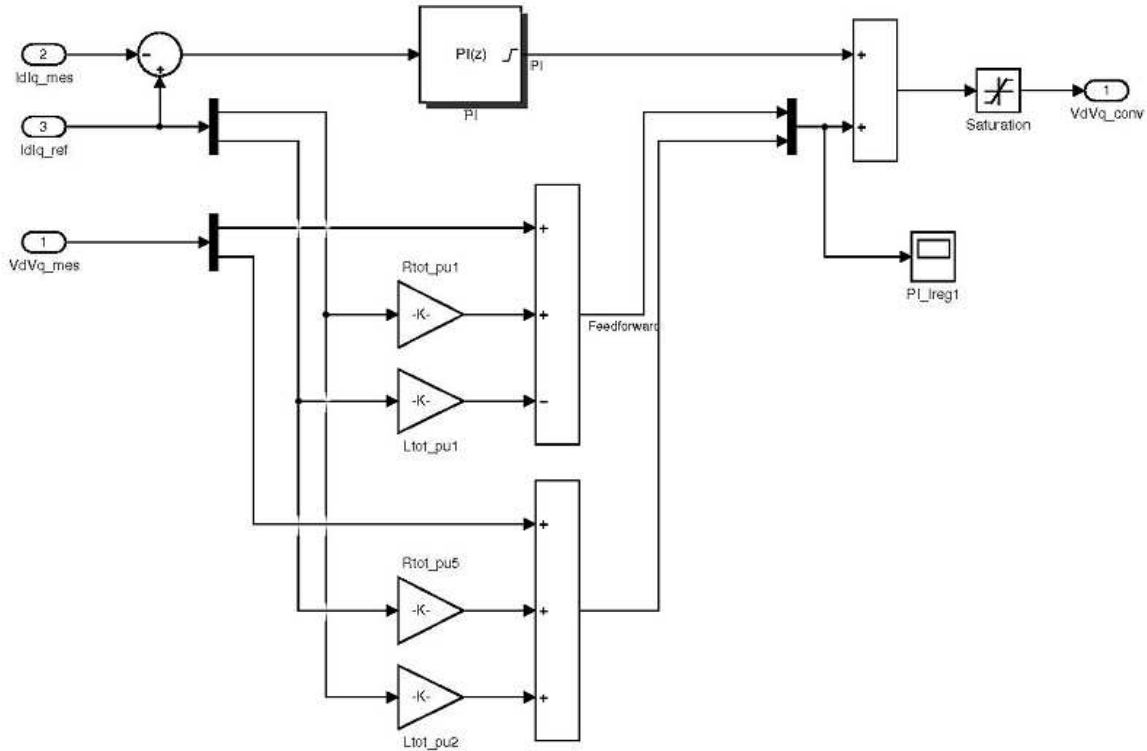


Fig: 5.8 Model of Current Regulator

Fig. 5.8 shows the block diagram of current regulator block.

Where

$$L_{tot} = L_x f_0 + L_{choke} \quad 5.1(a)$$

$$R_{tot} = R_x f_0 + R_{choke} \quad 5.1(b)$$

- L_x, R_x = Transformer leakage inductance and resistance
- L_{choke}, R_{choke} = inductance and resistance of series RL branch

$$V_{d(conv)} = V_{d(mes)} + I_d * R - I_q * L + L \frac{d}{dt} (I_d) \quad 5.2$$

$$V_{q(conv)} = V_{q(mes)} + I_d * L + I_q * R + L \frac{d}{dt} (I_q) \quad 5.3$$

Where

$V_{d(conv)}$ and $V_{q(conv)}$ are the converted voltage

V_d and V_q are the output signals of current controller which is converted to three modulating signals and it is delivered to pulse width modulation signal generator through a unit delay

keeping the modulation index (m) not greater than 1. Fig. 5.9 shows the detailed model of PWM generator block of the voltage source converter.

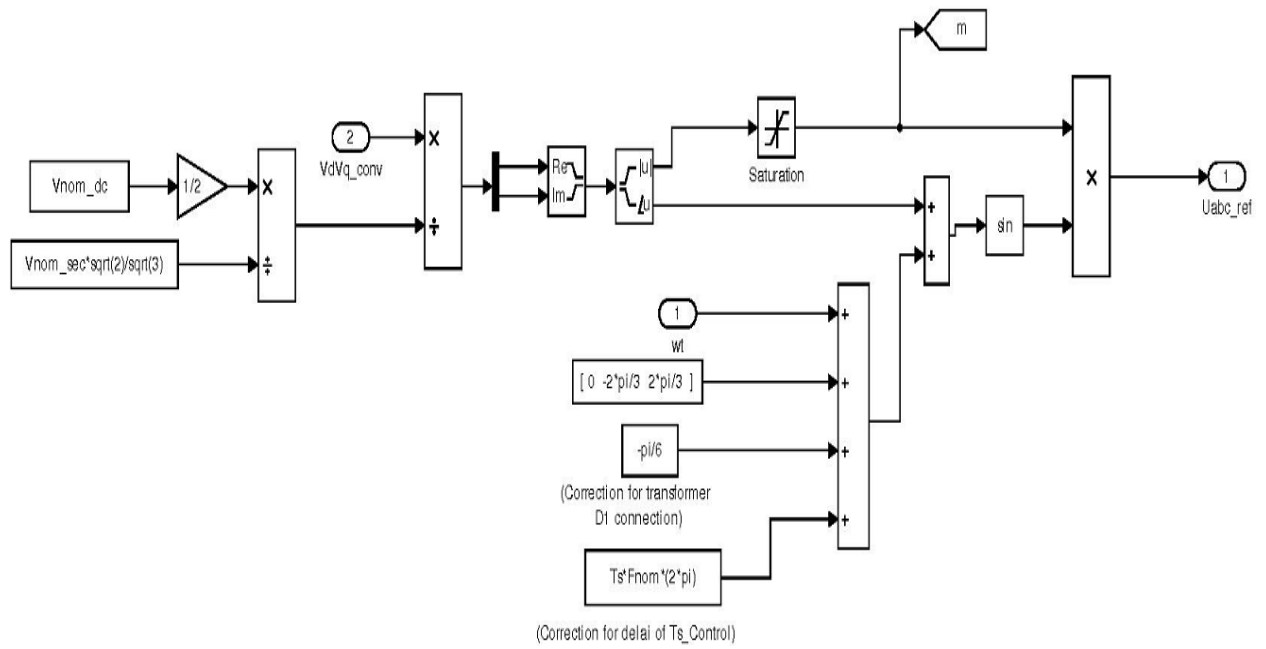


Fig: 5.9

CHAPTER 6

SIMULATION AND RESULTS

The photovoltaic model in chapter 2 is used to determine the performance of the photovoltaic system with boost converter and voltage sourced converter, while being connected to the utility grid. The following sections deal with each and every aspect of simulating the MPPT algorithm to the utility grid.

6.1 Simulation of MPPT Algorithms

In chapter 3 the Incremental Conductance MPPT algorithm was introduced and discussed. The following section describes the SIMULINK model of this method. The output of this MPPT algorithm controls the duty cycle of boost converter and thus helps in tracking the maximum obtainable power from the PV arrays under varying irradiance and temperature.

6.1.2 Incremental Conductance (INC) Method

Figure 6.1(a) and 6.1(b) shows the Simulink model of INC algorithm and the corresponding generation of pulses to control the DC-DC boost converter. The voltage and current obtained from the PV array are fed to the MPPT algorithm as input signals. The differential value of current and voltage is obtained by the Fourier transformation block of input signal. Simulink switches are employed here to route the signals in desired way by comparing them with their threshold value. In Fig 6.1 (a) we see that the derivative of input value along with mean value of the input quantities are fed to an addition block. After that a switching operation is performed. The value is then fed to a dead zone block to compare both the signals. After increasing the gain the output of the dead zone block is fed to discrete time integrator.

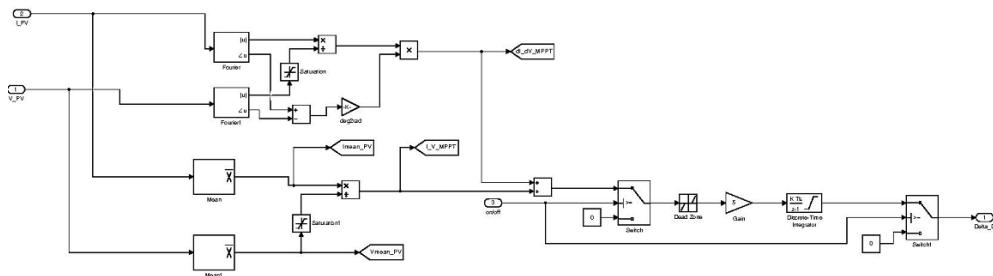


Fig: 6.1 (a)

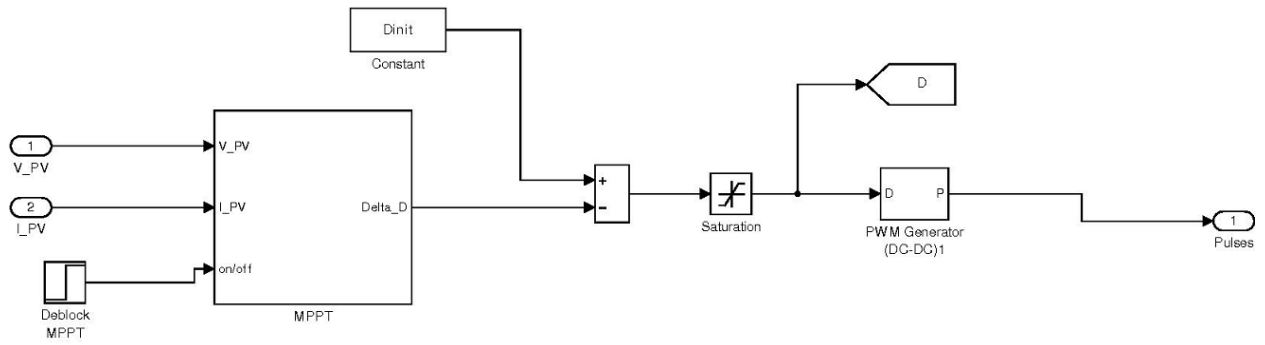


Fig: 6.1 (b) MPPT block for Incremental Conductance Method

The purpose of this integrator is to minimize the error $\left(\frac{dI}{dV} + \frac{I}{V}\right)$, thus making the sum as close to zero as possible and hence ensuring that the PV array always operates near the maximum power point. The on/off port takes input from the user and accordingly the user can operate maximum power tracker at desired time. In this case it is kept at 0.0 sec.

6.2 Simulation of Boost Converter

Fig 6.2(a) shows the Simulink model of boost converter. Photovoltaic output voltage is the input voltage to the boost converter. The MPPT controller sends the switching command to the transistor of the boost converter.

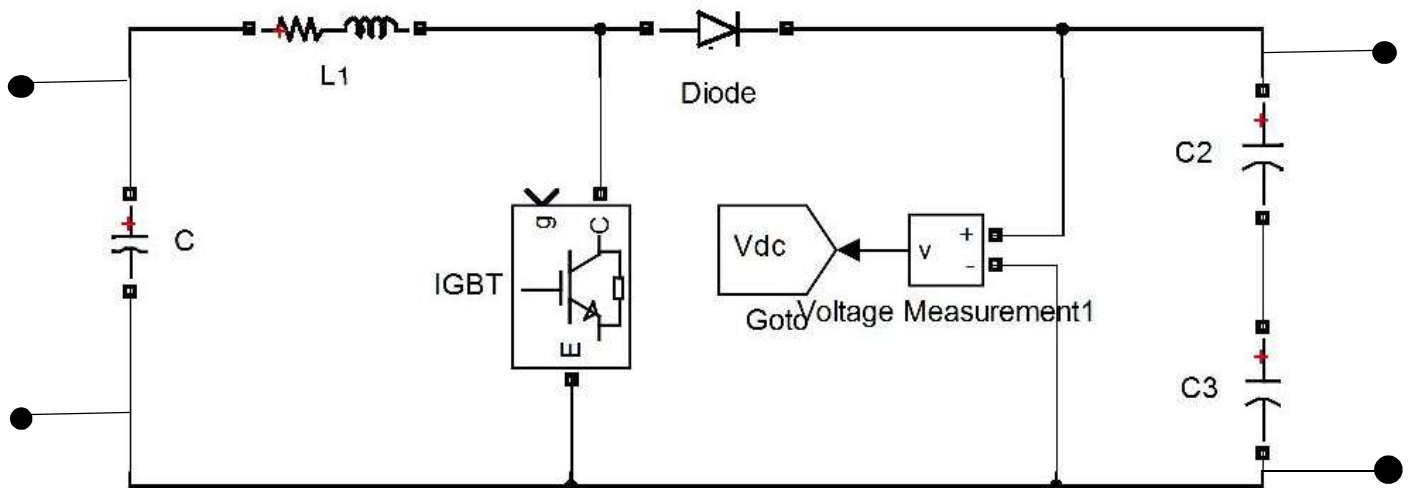


Fig: 6.2(a) DC-DC Boost Converter

The maximum power point controller block as used in the incremental conductance method is shown in figure 6.1 (b). The voltage and the current of the photovoltaic array are the input, and the duty cycle is the output. The duty cycle is compared to a saw tooth wave signal to

generate the PWM as shown in Fig 6.2 (b). The sampling frequency of the sawtooth waveform generator is 5000 Hz. The desired duty cycle can be entered into the PWM generator as can be seen from the Dinit block in Fig. 6.1(a). In our case the Dinit value is 0.5.

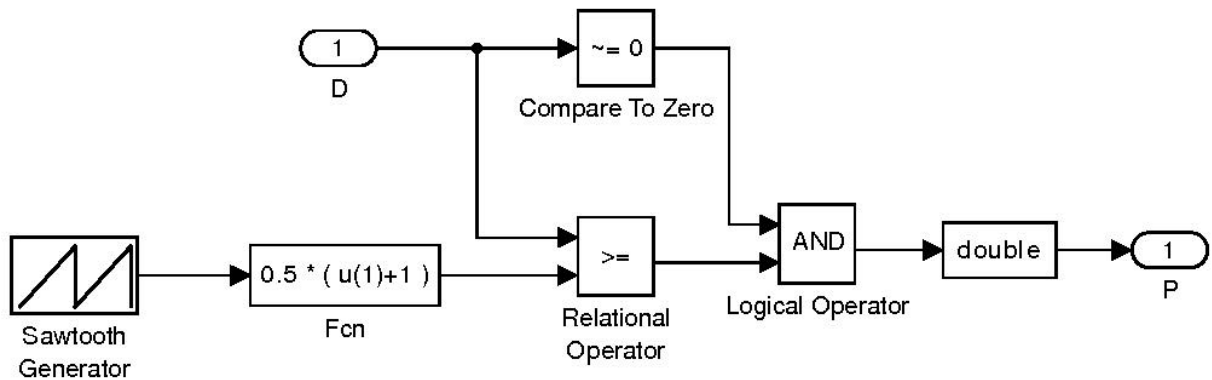


Fig: 6.2 (b)

6.3 Voltage Source Converter

Fig 6.3(a) shows the block diagram of PV array connected with the AC utility grid through an inverter topology and fig 6.3(b) shows the model of VSC control. These two models are already discussed in section 5.2 and 5.3 in chapter 5.

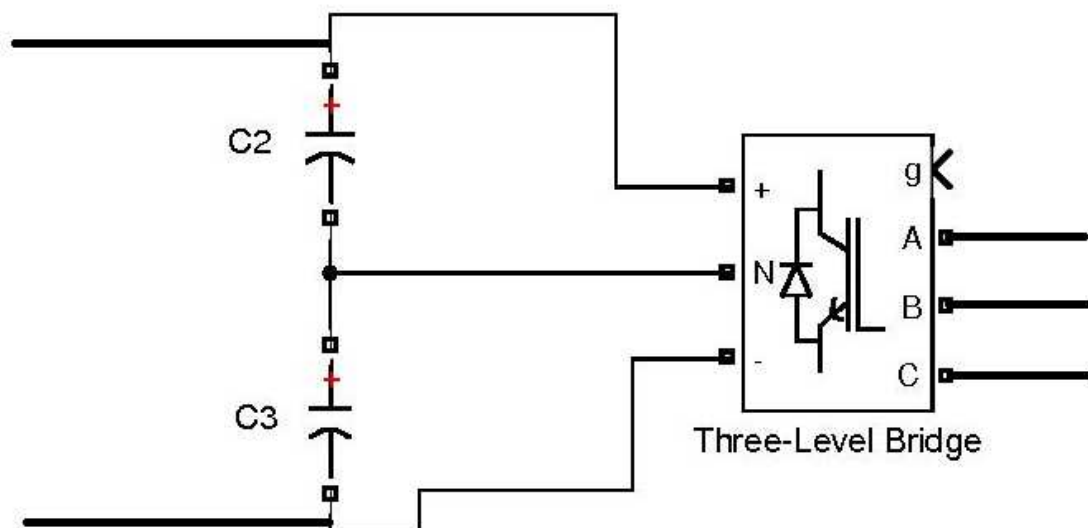


Fig: 6.3 (a) VSI

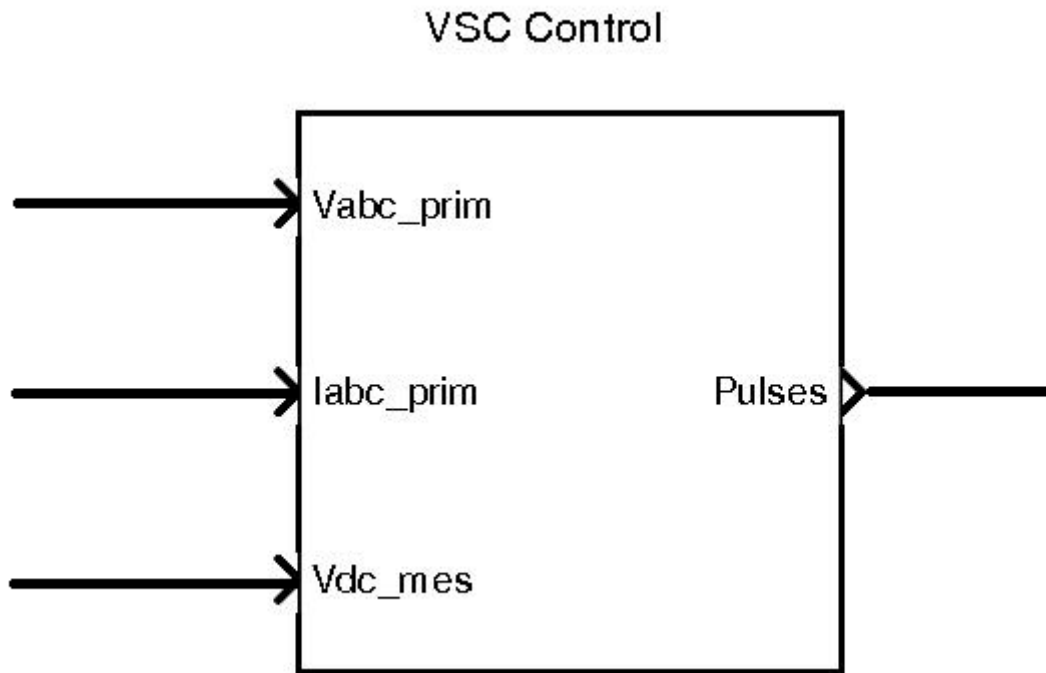


Fig: 6.3 (b)

6.4 Interfacing with AC Power Supply

The PV array is coupled with a boost converter. After that there is a power electronic interfacing which converts the DC quantity into AC value and is connected to the grid. This is seen in Fig 6.4 (a). As described earlier in chapter 5 section 5.1, the inductor reduces the ripple content of the inverter output voltage. The function of the capacitor bank in Fig. 6.4 (a) is to reduce the harmonic content of the inverter output voltage. Since the utility grid is a 10 MVA 50 Hz system hence the 240 V filtered inverter output voltage is stepped up to 11 kV through a 10 kVA, 50 Hz step up transformer.

Since the inverter output voltage will depend upon the voltage and current of the utility grid, hence some sort of feedback mechanism is required. This is seen in Fig. 6.3 (b). The Simulink model that measures the power voltage and current fed to the AC supply is shown in Fig 6.4 (a). The three phase voltage and current at block B1 is fed to a power positive sequence block to get the active and reactive power. A termination block is used here to terminate the reactive power signal. Two selector block is used to get the voltage and current of a particular phase. This is shown in Fig. 6.4 (b).

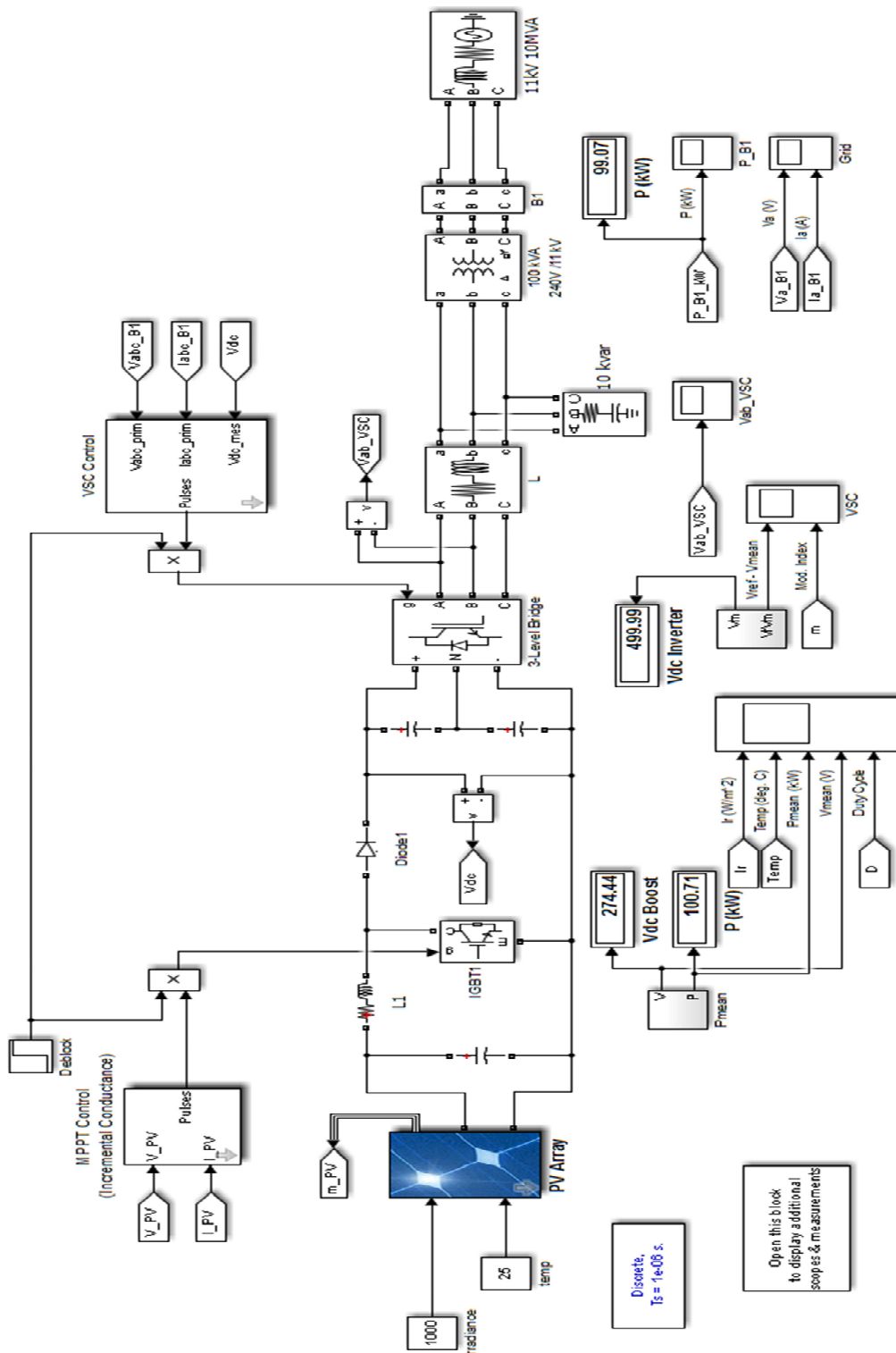


Fig: 6.4 (a) Simulation model of PV array connected to utility grid.

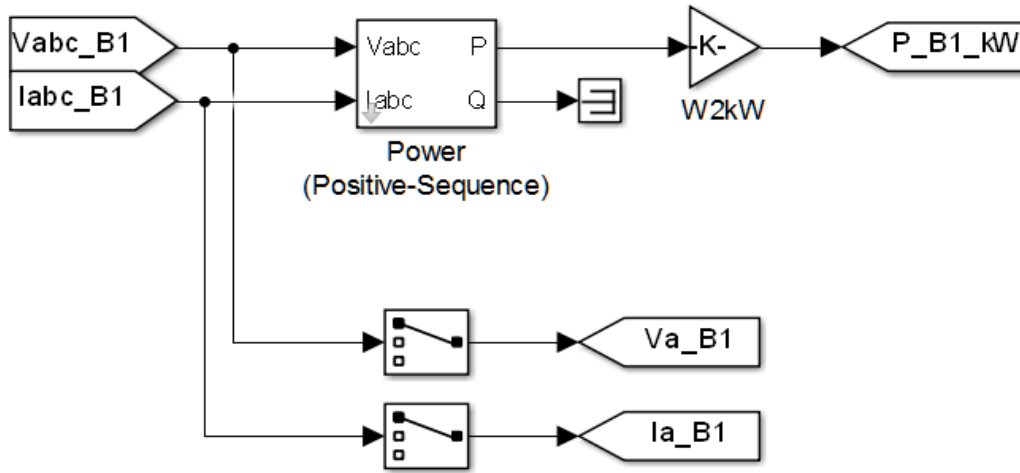


Fig: 6.4 (b)

6.5 Result & Discussions

The simulation presents an analysis of the PV array of 100 kW with boost converter connected with utility supply. The PV system parameter is already mentioned in Table 2.1 in chapter 2. Simulation run time 2.5 seconds. Sampling time is $1\mu s$.

6.5.1 Power obtained from PV array

At the beginning of simulation the sun irradiation is set at $G= 1000W/m^2$ and temperature is set at $25^{\circ}C$. The desired output power of PV array should be 100 kW at $1000W/m^2$ irradiance and 500 W at $500W/m^2$ irradiance. This has been achieved by our simulation model as shown in Fig. 6.5 (a).

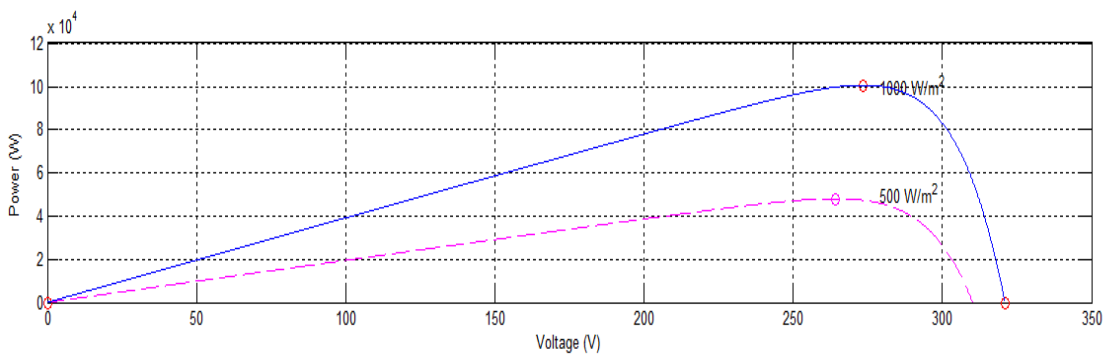


Fig: 6.5 (a)

At the end of simulation the PV array generates around 100.71 kW power at an irradiance of 1000W/m^2 and at temperature of 25°C . With the variation in temperature it may vary. Fig 6.5 (b) represents the output power of PV array.

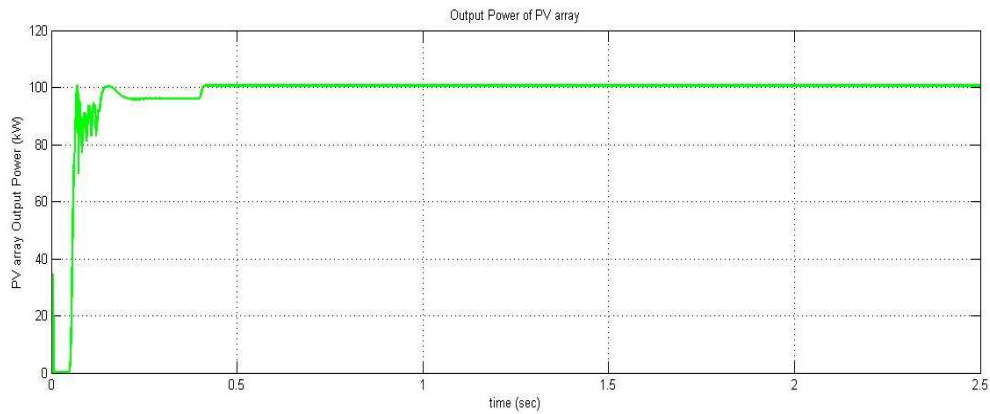


Fig: 6.5 (b)

Fig. 6.5 (c) represents the PV array mean voltage. At end of simulation the PV mean voltage is 274.44 V.

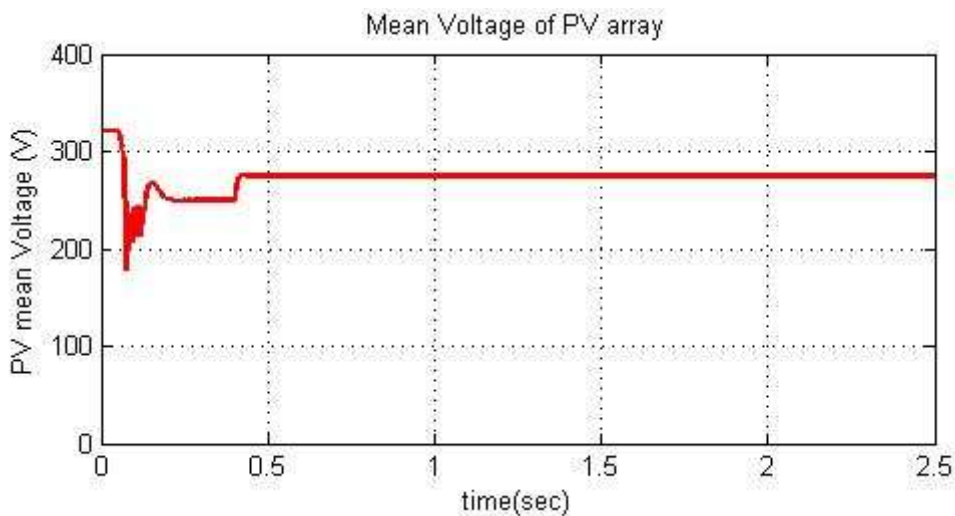


Fig 6.5(c)

Fig 6.5 (d) represents the duty cycle which is being used to generate pulses to control the DC-DC boost converter. There is a change in the duty cycle after 0.4 sec because at this moment the MPPT controller comes into operation and tracks the maximum power point but since the irradiance is constant, after this moment there is no change in the duty cycle and it remains fixed as shown in Fig. 6.5 (d).

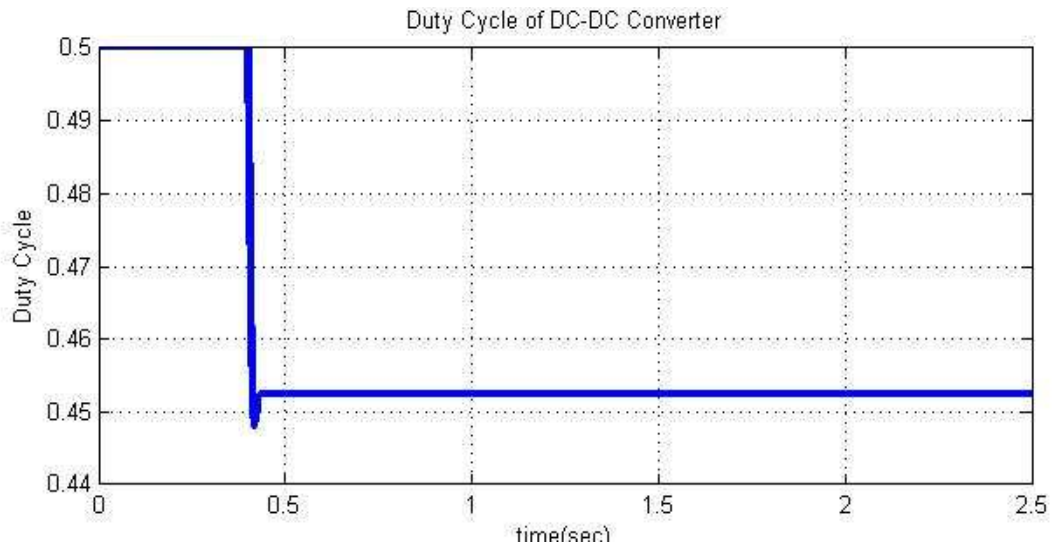


Fig: 6.5(d)

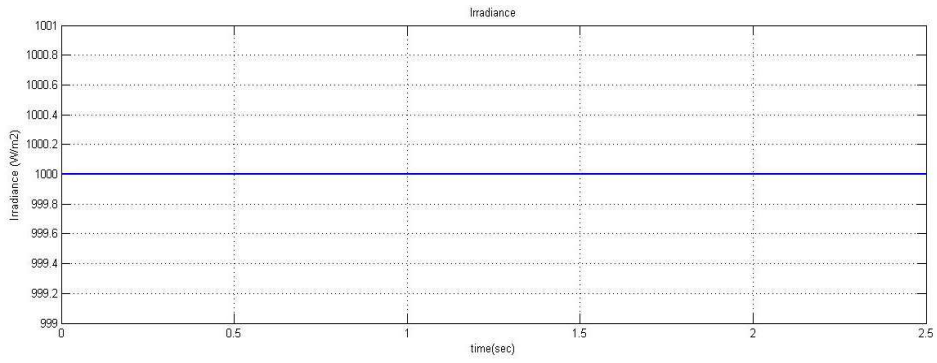


Fig: 6.5 (e)

Fig. 6.5 (e) represents the irradiance. It shows that the irradiance is set at 1000kW/m² for this simulation.

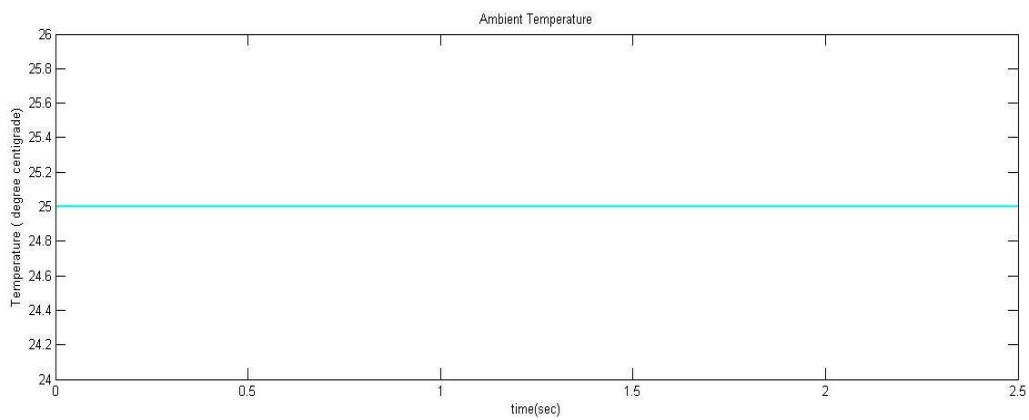


Fig: 6.5 (f)

Fig. 6.5 (f) represents the ambient temperature of the PV array. It can be seen that the temperature of the PV array is kept fixed at 25°C.

6.5.2 Voltage Source Converter output

Fig 6.5 (g) shows the output of voltage source converter. The output voltage of Voltage source converter (VSC) is around the 500 V voltage mark as prescribed by the output of the boost converter.

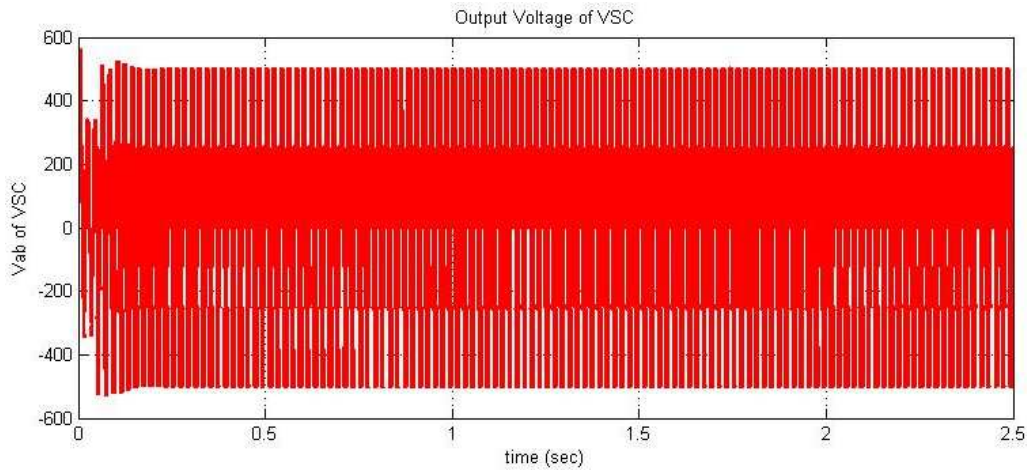


Fig 6.5 (g)

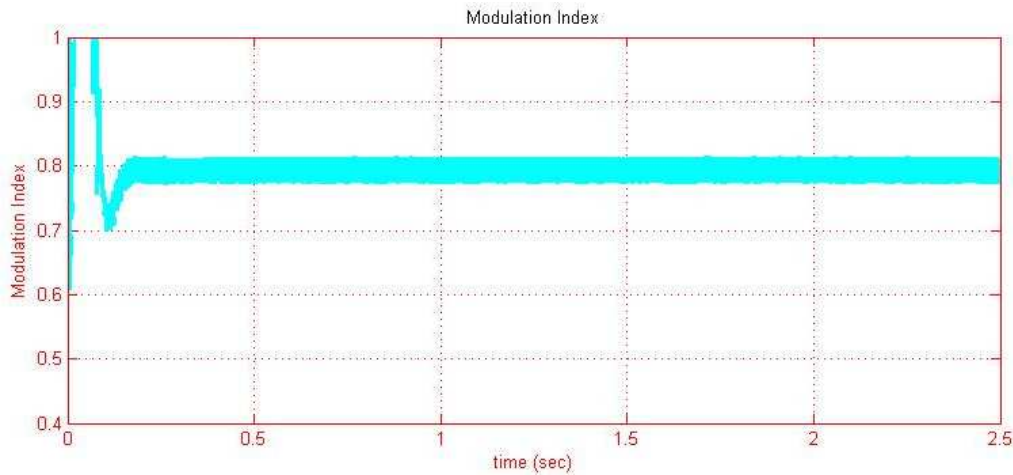


Fig: 6.5 (h)

Modulation index is the ratio of peak magnitudes of the modulating waveform and the carrier waveform. It relates the inverter's dc-link voltage and the magnitude of pole voltage (fundamental component) output by the inverter. It must not be greater than 1. Fig. 6.5 (h) represents the modulation index of the inverter and it is found that the modulation index is well below 1 thus validating our design.

Fig 6.5(i) represents the power input in kW which is fed to the AC supply. It can be shown from the figure that the PV array will deliver 99.07 kW power to the utility grid. The figure shows the amount of power delivered to the utility grid.

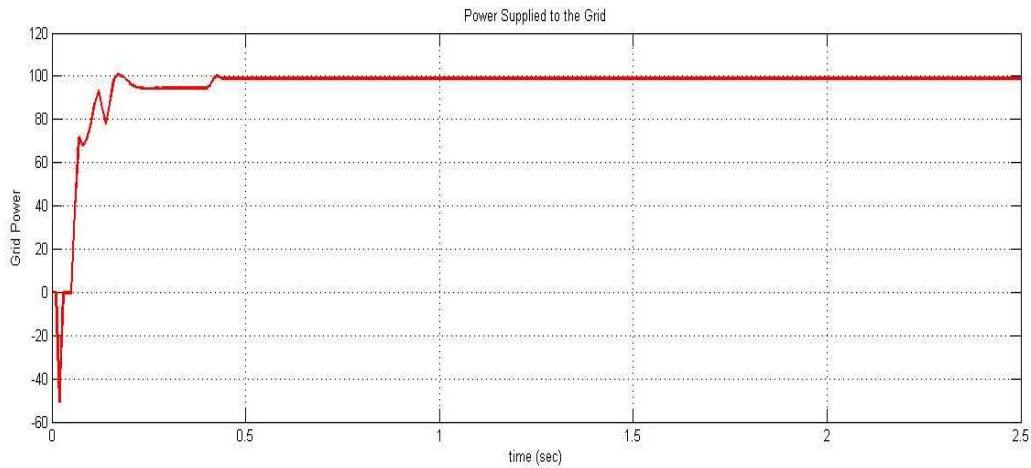


Fig. 6.5 (i)

The irradiance is then varied as shown in Fig. 6.5(j) and the ambient temperature is kept constant at 25° C. The MPPT controller block of the PV array is able to track the available maximum power point irrespective of the variation in the irradiance and thus provide the grid with the required amount of power. This is shown in Fig. 6.5 (k).

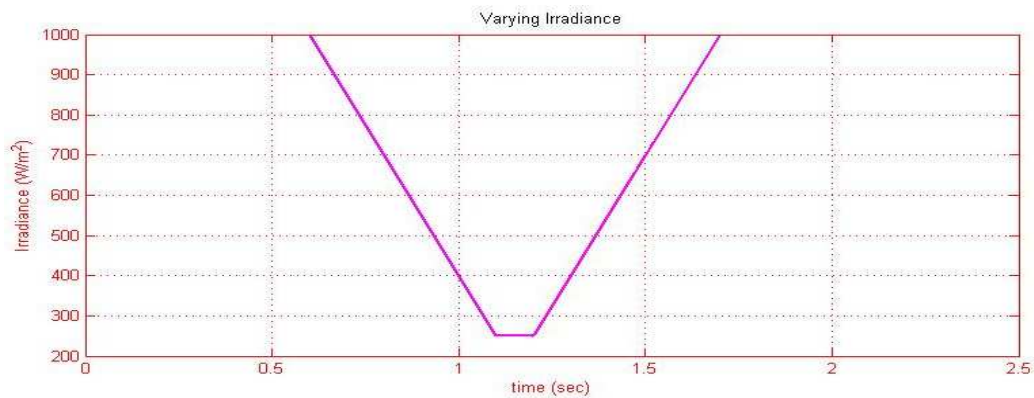


Fig. 6.5 (j)

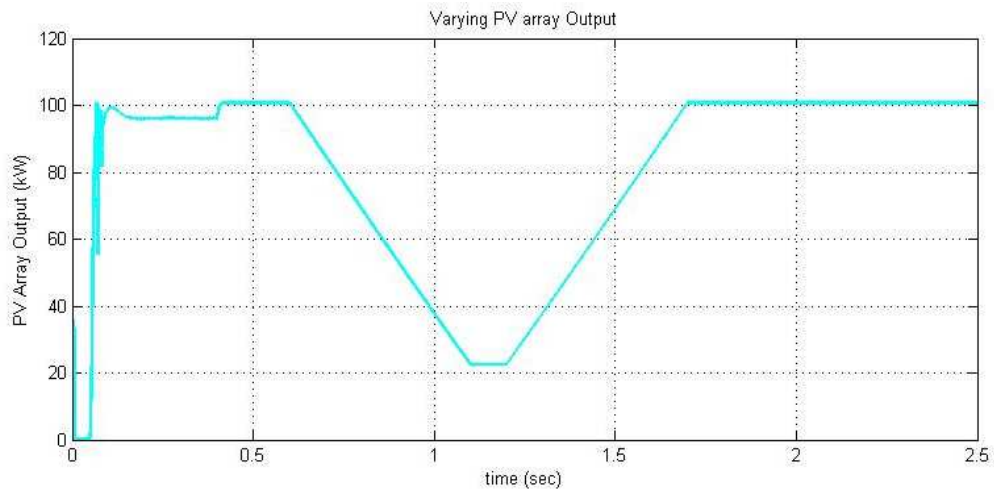


Fig. 6.5 (k)

Correspondingly the voltage output of the PV array is also varying along with the duty cycle of the DC-DC boost converter. Fig. 6.5 (l) and Fig. 6.5 (m) are showing these two features.

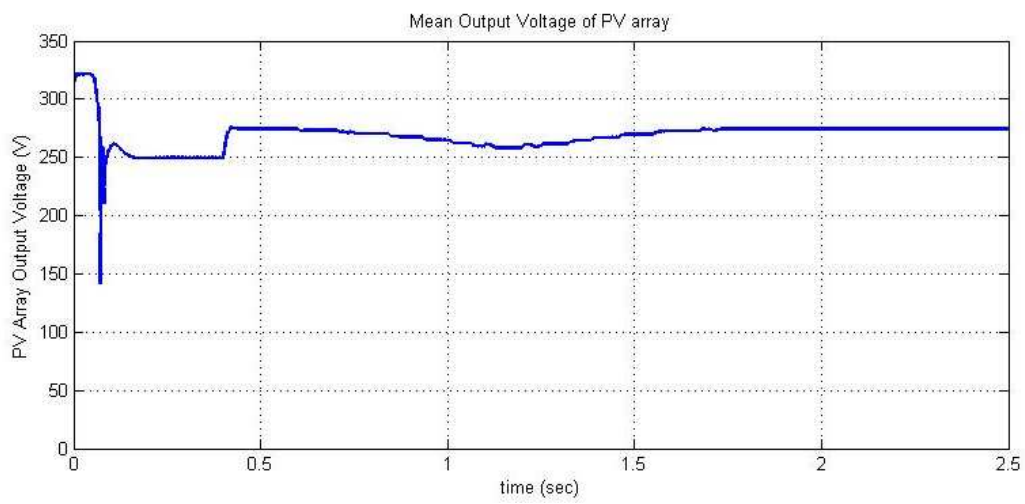


Fig. 6.5 (l)



Fig. 6.5 (m)

Figure 6.5 (n) shows the variation in the power input to the grid.

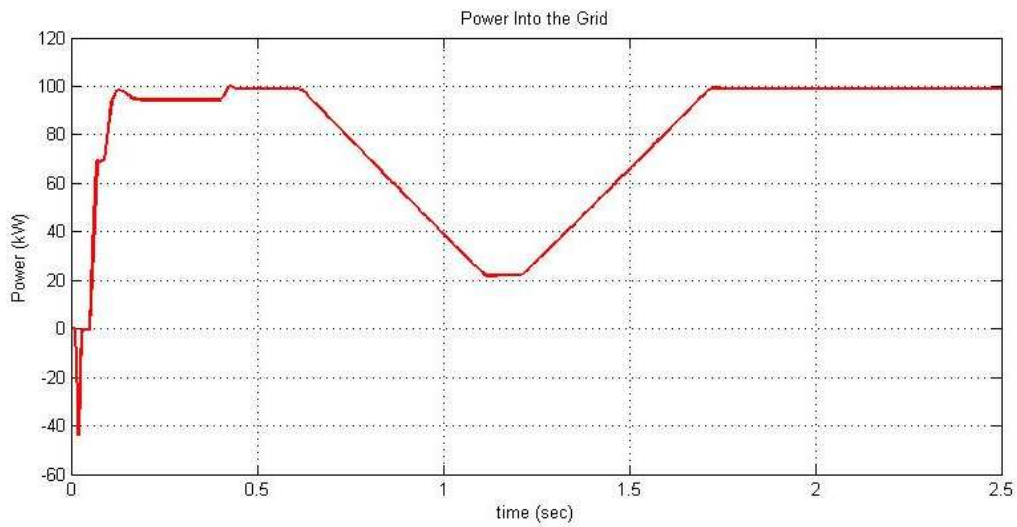


Fig. 6.5 (n)

The figures above clearly describe that our objective has been achieved. The PV array designed is giving the desired result of 100.71 kW power into the grid and the grid is receiving a power of 99.07 kW. The only drawback of this simulation is that the filtered inverter output voltage has a higher THD than the allowable value. This is shown in Fig. 6.5 (o).

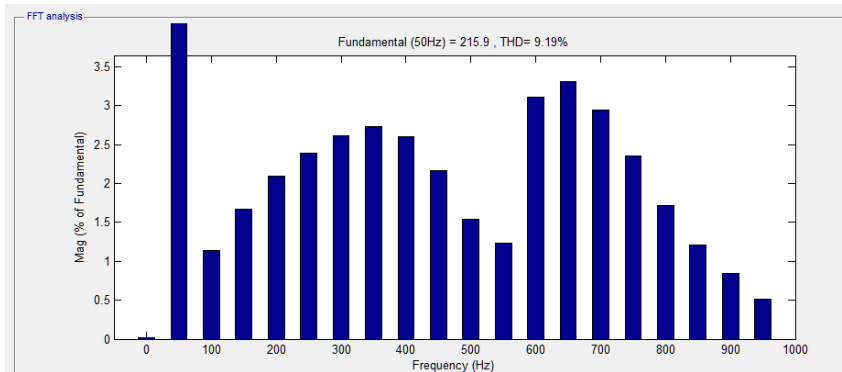


Fig. 6.5(o)

CHAPTER 7

CONCLUSION AND SCOPE OF FUTURE WORK

7.1 Conclusion

In this thesis, modeling of grid connected PV array using SIMULINK/MATLAB has been carried out. Modeling of an accurate PV cell has always appeared as a challenge, more so when the PV module is used to simulate PV arrays and PV Panels. This research addresses both issues by simulating a comprehensive model in Simulink that takes into consideration the most important elements in a PV cell, array or panel. From the theory of the photovoltaic cells, a mathematical model of the PV array has been presented. The model is entirely based on the datasheet parameters given by the manufacturer. Then, the photovoltaic systems with DC-DC boost converter, maximum power point controller connected to AC supply through a voltage source converter have been designed. Finally, the system has been simulated with Simulink /MATLAB.

The simulation of the PV panels shows that the simulated models are accurate to determine the voltage current characteristics of commercially available PV panels as the characteristics obtained from simulation are almost the same as given in the manufacturer's datasheet. In addition, with change in the irradiance or temperature, the PV array models output voltage and current also changes in accordance with the desired performance. The simulation shows that the Incremental Conductance algorithm can track the maximum power point of the PV array and it always run at maximum power point under varying operating conditions. The results showed that the algorithm delivered efficiency close to 100% in steady state.

The contribution of this thesis includes the following:

1. Design of Simulink PV module.
2. MPPT method is coupled with a DC-DC boost converter in Simulink.
3. Implementation of voltage source converter and its control using the PLL block.
4. Model validation.

7.2 Future Scope of Work

The Simulink model of the PV array could be used in the future for extended study with different MPP methods and DC/DC converter topology. Different type of voltage control methods can be implemented to keep the boost converter output voltage ripple free. The simulation of PV system with various types of inverter topologies for grid interfacing can be

investigated. Apart from the VSI topology the CSI topology can also be investigated and corresponding PWM techniques can also be developed.

Since the power electronic interfacing uses power electronic switches hence the effect of harmonics on the grid voltage can be studied in regard to the connection of PV system with the grid as the ultimate goal of each and every utility is to supply its consumer with the best quality power.

The PV interfacing that we have studied is a stand-alone system. The same PV module can be utilized to charge a battery bank and then can be interfaced with the utility grid. This increases the reliability of the PV systems. Many research areas are being directed to this particular aspect.

Further studies can still be done with PV system for research purposes and a detailed PV simulator might be useful for educational and laboratory purposes.

Bibliography

- [1] <http://energy.gov/oe/services/technology-development/smart-grid/role-microgrids-helping-advance-nation-s-energy-system>
- [2] https://en.wikipedia.org/wiki/Solar_power_in_India
- [3] www.eai.in/ref/ae/sol/sol.html
- [4] www.renewableenergyworld.com/index/tech.html
- [5] Mohamed A. Eltawil and Zhengming Zhao “Grid-connected photovoltaic power systems: Technical and potential problems- A review” Renewable and Sustainable Energy Reviews 14 (2010) 112-129.
- [6] Gokay Bayrak and Mehmet Cebeci “Grid connected fuel cell and PV hybrid power generating system design with Matlab Simulink. International Journal of Hydrogen Energy 39 (2014) 8803-8812.
- [7] M. Sujith, R Mohan and P. Sundravadeivel “Simulation Analysis of 100kW Integrated Segmented Energy Storage for Grid Connected PV System. International Journal of Electrical Engineering & Technology (IJEET). Vol. 3 July-September (2012) pp. 164-173.
- [8] Moacyr Aurliano Gomes de Brito, Luigi Galotto, Jr., Leonardo Poltronieri Smapaio, Guilherme de Azevedo e Melo and Carlos Alberto Canesin “Evaluation of the Main MPPT Techniques for Photovoltaic Applications” IEEE Transaction on International Electronics, Vol. 60, No. 3 March 2013.
- [9] Zhao Dongemi, Zhang Nan and Liu Yanhua “Micro-grid Connected/Islanding Operation Based on Wind and PV Hybrid Power System” IEEE PES ASGT ASIA 2012 1569527723.
- [10] I. H. Atlas and A. M. Sharaf “A Photovoltaic Array Simulation Model for Matlab-Simulink GUI Environment” Clean Electrical Power. 2007. ICCEP '07. International Conference on. Publication Year: 2007. Pages 341-345.
- [11] Habbati Bellia, Ramdani Youcef and Moulay Fatima “A detailed modeling of photovoltaic module using Matlab” NRIAG Journal of Astronomy and Geophysics 2014, 3 pages 53-61

- [12] Chen Qi, Zhu Ming “Photovoltaic Module Simulink Model for a Stand-alone PV System” 2012 International Conference on Applied Physics and Industrial Engineering. Pages 94-100
- [13] Michael E. Ropp “Development of a Matlab/Simulink Model of a Single-Phase Grid -Connected Photovoltaic System” IEEE Transactions on Energy Conversion 2009.
- [14] [cial.aero/Pressroom/newsdetials.aspx?news_id=360](http://www.faa.gov/cial/aero/Pressroom/newsdetials.aspx?news_id=360)
- [15] Shivananda Pukhrem “A Photovoltaic Model with Matlab/Simulink”.
- [16] Yushaized Yusof, Siti Hamizah Sayuti, Muhammad Abdul Latif and Mohd. Zamri Che Wanik “Modeling and Simulation of Maximum Power Point Tracker for Photovoltaic System” National Power & Energy Conference (PECon) 2004 Proceedings, Kuala Lumpur, Malaysia.
- [17] Geoffrey R. Walker “Cascaded DC-DC Converter Connection of Photovoltaic Modules” IEEE Transactions on Power Electronics, Vol. 19 No. 4 July 2004.
- [18] Mamadou Bailo Camara, Hamid Gualous, Frederic Gustin, Alain Berthon “DC/DC Converter Design for Supercapacitor and Battery Power Management in Hybrid Vehicle Applications-Polynomial Control Strategy” IEEE Transaction on Industrial Electronics Vol. 57 No 2 February 2010.
- [19] Nitin P. Choudhury and Prof. Xma R. Pote “Controlling of Back to Back Converter for Load Sharing in Microgrid and Utility Grid” 2013 Third International Conference on Advances in Computing and Communications
- [20] A. Safari and S. Mekhilef “Incremental Conductance MPPT Method for PV Systems” IEEE CCECE 2011
- [21] Saravana Selvan. D “Modeling and Simulation of Incremental Conductance MPPT Algorithm for Photovoltaic Applications” International Journal of Scientific Engineering and Technology Vol. No. 2 Issue No. 7, pp 681-685 1 July 2013.
- [22] M.A.A: Mohd Zainuri, M.A. Mohd Radzi, Azura Che Soh and N. Abdul Rahim “Adaptive P & O – Fuzzy Control MPPT for PV Boost Dc-Dc Converter” 2012 IEEE International Conference on Power and Energy.

- [23] Hassan Fathabadi “Novel high efficiency DC/DC boost converter for using in photovoltaic systems” *Solar Energy* 125 (2016) 22-31 ELSEVIER.
- [24] B. M Hasaneen and Adel A. Elbaset Mohammed “Design and Simulation of DC/DC Converter” 978-1-4244-1933 2008 IEEE.
- [25] P. Sathya, Dr. R Natarajan “Design and Implementation of 12V/24V Closed loop Boost Converter for Solar Powered LED Lighting System” *International Journal of Engineering and Technology. (IJET)* Vol 5 No 1 Feb-Mar 2013
- [26] Neng Cao, Yajun Cao and Jiaoyu Liu “Modeling and Analysis of Grid- Connected Inverter for PV Generation” 2nd International Conference on Computer Science and Electronics Engineering
- [27] Yao-Nan Tong, Chun-Lai Li and Feng Zhou “Synchronization control of single-phase full bridge photovoltaic grid-connected inverter.” *Optik* 127 (2016) 1724-1728
- [28] Amirnaser Yazdani, Reza Iravani “Voltage Sourced Converter”
- [29] Tarak Salmi, Mounir Bouzguenda, Adel Gastli and Ahmed Masmoudi “Matlab/Simulink Based Modelling of Solar Photovoltaic Cell” *International Journal of Renewable Energy Research. Vol. 2 No. 2* 2012
- [30] Savita Nema, R. K. Nema and Gayatri Agnihotri “Matlab/Simulink based study of photovoltaic cells / modules / array and their experimental verification” *International Journal of Energy and Environment Vol. 1 No. 3 pp 487-500, 2010*
- [31] “TRENDS IN PHOTOVOLTAIC APPLICATIONS Survey report of selected IEA countries between 1992 and 2010”, International Energy Agency, Report IEA-PVPS T1-20:2011 [Online].
Available:http://www.ieapvps.org/products/download/Trends-in-Photovoltaic_2010.pdf
- [32] Azevedo G. M. S, Cavalcanti M. C. Oliviera K. C., Nevas F. A. S., and Lins Z. D. “Evaluation of maximum power point tracking methods for grid connected photovoltaic systems,” *Conference on Power Electronics Specialists, 2008. PESC 2008. IEEE, August 2008, pp. 1456 - 1462.*
- [33] Trishan ESRAM “Comparison of Photovoltaic Array Maximum Power Point Tracking Techniques” *IEEE Transactions on Energy Conversion, Vol. 22, No. 2, June 2007.*
- [34] Moahn Ned, Undeland Tore M. and Robbins William P. “Power Electronics, Converter Applications and Design” John Willey & Sons.
- [35] S. B. Kajer, J. K. Pederson and F. Blaabjerg, “Power inverter topologies for PV modules- a review” in *Proceedings IEEE-IAS Annual meeting, vol. 2, 2002 pp. 782-788. 15*

- [36] B. Farhangi and S. Farhangi, "Comparison of Z-source inverter and buck boost topologies as a single phase transformer less photovoltaic grid connected power conditioner", in Power Electronics Specialist Conference, 2006, pp 1-6
- [37] M. Kazerani and Y. Ye "Comparative evaluation of three phase PWM voltage and current-source converter topology in FACTS application", in PES general meeting 2002 pp. 473-479
- [38] M. H. Bierhoff and F. Fuchs, "Semiconductor losses in voltage source and current source IGBT converter based on analytical derivation", in PES Conference, vol. 4
- [39] M. Mohr and F. Fuchs, "Comparison of three-phase current source inverters and voltage source inverters linked with dc-dc boost converters for fuel cell generation systems" in European Conference on power electronic application, 2005, pp. 10
- [40] Rashid Muhammad H. "Power Electronics: Circuits, Device, and Applications" Pentice Hall of India.

APPENDIX A

MANUFACTURER DATASHEET

SUNPOWER™

E18 / 305 SOLAR PANEL

EXCEPTIONAL EFFICIENCY AND PERFORMANCE

BENEFITS

Highest Efficiency

SunPower™ Solar Panels are the most efficient photovoltaic panels on the market today.

More Power

Our panels produce more power in the same amount of space—up to 50% more than conventional designs and 100% more than thin film solar panels.

Reduced Installation Cost

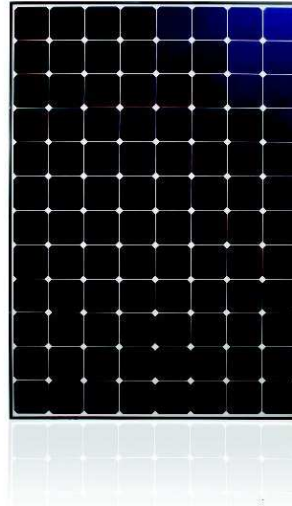
More power per panel means fewer panels per install. This saves both time and money.

Reliable and Robust Design

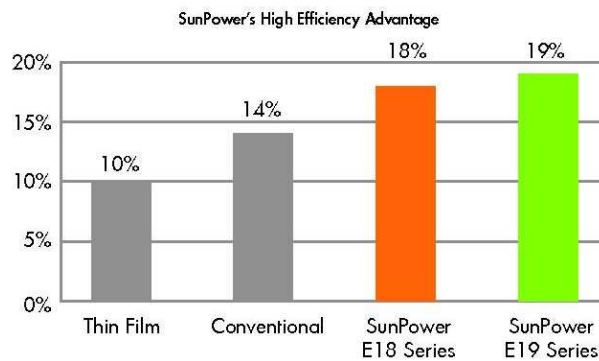
Proven materials, tempered front glass, and a sturdy anodised frame allow panel to operate reliably in multiple mounting configurations.



SPR-305E-WHT-D



The SunPower™ 305 Solar Panel provides today's highest efficiency and performance. Utilising 96 SunPower all back-contact solar cells, the SunPower 305 delivers a total panel conversion efficiency of 18.7%. The 305 panel's reduced voltage-temperature coefficient, anti-reflective glass and exceptional low-light performance attributes provide outstanding energy delivery per peak power watt.



Electrical Data

Measured at Standard Test Conditions (STC): Irradiance 1000W/m², AM 1.5, and cell temperature 25° C

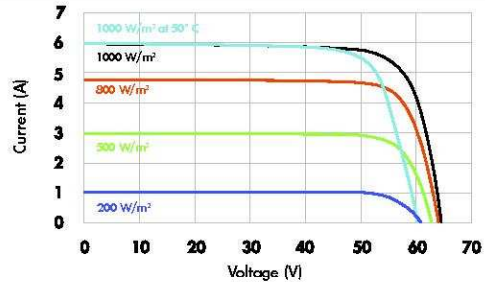
Nominal Power (+5/-3%)	P _{nom}	305 W
Efficiency	η	18,7 %
Rated Voltage	V _{mpp}	54,7 V
Rated Current	I _{mpp}	5,58 A
Open Circuit Voltage	V _{oc}	64,2 V
Short Circuit Current	I _{sc}	5,96 A
Maximum System Voltage	IEC	1000 V
Temperature Coefficients	Power (P)	-0,38% / K
	Voltage (V _{oc})	-176,6mV / K
	Current (I _{sc})	3,5mA / K
NOCT		45° C +/-2° C
Series Fuse Rating		15 A
Limiting Reverse Current (3-strings)	I _r	14,9 A

Electrical Data

Measured at Nominal Operating Cell Temperature (NOCT): Irradiance 800W/m², 20° C, wind 1 m/s

Nominal Power	P _{nom}	227 W
Rated Voltage	V _{mpp}	50,4 V
Rated Current	I _{mpp}	4,49 A
Open Circuit Voltage	V _{oc}	60,1 V
Short Circuit Current	I _{sc}	4,82 A

I-V Curve



Current/voltage characteristics with dependence on irradiance and module temperature.

Tested Operating Conditions

Temperature	-40° C to +85° C
Max load	550 kg / m ² (5400 Pa), front (e.g. snow) w / specified mounting configurations 245 kg / m ² (2400 Pa) front and back - e.g. wind
Impact Resistance	Hail - 25 mm at 23 m/s

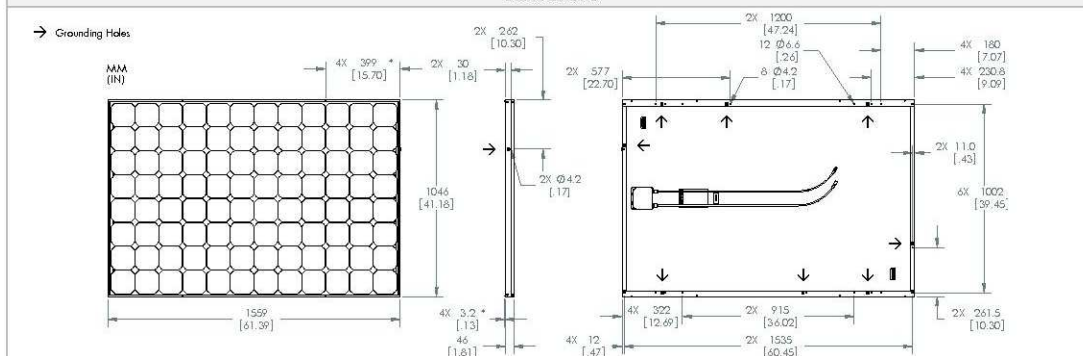
Warranties and Certifications

Warranties	25 year limited power warranty 10 year limited product warranty
Certifications	IEC 61215 Ed. 2, IEC 61730 (SCL1)

Mechanical Data

Solar Cells	96 SunPower all-back contact monocrystalline	Output Cables	1000mm length cables / MultiContact (MC4) connectors
Front Glass	high transmission tempered glass with anti-reflective (AR) coating	Frame	Anodised aluminium alloy type 6063 (black)
Junction Box	IP-65 rated with 3 bypass diodes 32 x 155 x 128 (mm)	Weight	18,6 kg

Dimensions



CAUTION: READ SAFETY AND INSTALLATION INSTRUCTIONS BEFORE USING THE PRODUCT.

Visit sunpowercorp.com for details

SUNPOWER and the SUNPOWER logo are trademarks or registered trademarks of SunPower Corporation.
© September 2010 SunPower Corporation. All rights reserved. Specifications included in this datasheet are subject to change without notice.

sunpowercorp.com
Australia: sunpowercorp.com.au
Document #001-64025 Rev** / A4_EN